Homonuclear Recoupling and Heteronuclear Decoupling

Using Combination of Exponentially Modulating Fields and Symmetry Based Pulse Sequences

---

A thesis submitted towards partial fulfillment of
BS-MS programme dual degree program
by

Sheetal kumar Jain
Under the guidance of
Professor Niels Christian Nielsen
Director of Center for Insoluble Protein Structures (inSPIN)
Interdisciplinary Nanoscience Center (iNANO) and
Department of Chemistry, University of Aarhus

Department of Physics
Indian Institute of Science Education and Research Pune

Certificate

This is to certify that this dissertation entitled 'Homonuclear Recoupling and Heteronuclear Decoupling Using Combination of Exponentially Modulating Fields and Symmetry Based Pulse Sequences' submitted towards the partial fulfillment of the BS-MS dual degree programme at the Indian Institute of Science Education and Research, Pune represents original research carried out by Sheetal Kumar Jain at University of Aarhus, Denmark under the guidance of Prof. Niels Christian Nielsen during the academic year 2010-2011.

Signature of student:

Supervisor:	Head Physical Sciences:
Date:	Date:
Place: Aarhus	Place: Pune

List of Projects and Publications

.

Projects:

1. Composite Pulses and Decoupling In Liquid State NMR, with Dr. T.S. Mahesh.
2. Preparation of Pseudo-pure States in NMR-QIP, with Dr. T.S. Mahesh.
3. Mathematical Analysis of the MEGA-PRESS Pulse Sequence for Different Spin Systems, with Dr. Pravat Mandal.

Publications:

1. Nielsen, A. B.; Jain, S. K. & Nielsen, N. C. "Low-power homonuclear dipolar recoupling using supercycled symmetry-based and exponentially-modulated pulse sequences." Chemical Physics Letters, 2011, 503, 310-315

Acknowledgements

During my masters I have been fortunate to meet and work with many wonderful people. At IISER Pune, I had many chances to listen great scientists of the world and to learn from outstanding teachers. I am thankful to all my teacher during this time for giving insight of many fundamentals of science specially physics and maths. I owe my deepest gratitude to Dr. T.S. Mahesh for introducing me to NMR. Projects, completed under his guidance, are of great importance for the future of my research in this field.
I earned great friends at IISER who did not only made these years amusing but also supported me and provided valuable suggestions when needed.
The last year of my masters has been a great experience for me. It was an auspicious time to work under Prof. Niels Chr. Nielsen and it is an honor for me to be a part of his group. I am grateful to my supervisor for assigning me an elucidative project, full of opportunities to learn exciting theories and experimental techniques. I would like to thank him for his kind instructions and favors during my stay in Denmark.
I am also thankful to Prof. Navin Khaneja for having important discussions with me during this project. It was a pleasant coincident that he was in Denmark as a guest professor in Prof. Nielsen's group for the same period of my project and I had a golden opportunity to interact with him.
I want to convey my hearty thanks to all the inSPIN group members for providing me an amicable atmosphere. Anders Bodholt and Lasse Arnt Straasø made available their supports in number of ways. They helped me with the use of the spectrometer, discussed basic theories and made my stay comfortable by guiding me for all the practical purposes in this country. I am indebted to Lasse for getting some time for proof reading of this thesis out of his very busy schedule. I am obligated to Katrine, Jacob, Gabriel, Jokim, Mads, Morten, Moks, Nataliya, Berit, Kresten and all the others for making this time better by their warm treatments.
I am indebted to my friends Sushant, Anand and Ajit for their encouraging remarks and debates on different concepts.
Finally, I would like to say thanks to my family for their blessings and support without which it would not have been possible to complete this thesis.

Abstract

Nuclear magnetic resonance is a technique with a wide range of applications in biological and chemical sciences. Developments in the methods for recoupling and decoupling in solid-state nuclear magnetic resonance are of fundamental importance for its use in studying the biomolecules. In this thesis, work on developing such pulse sequences is presented. For recoupling, symmetry-based pulse sequences (CN_n^ν and RN_n^ν)are well known and frequently used. Exponentially modulating recoupling technique is a sequence which make use of a small oscillating field in addition to a comparatively strong rf field to recouple effectively at low power irradiation. Inspired by strong points of these two techniques, here we present a new method EXPORT-CN. This offers an effective recoupling at low power and at high spinning conditions. Some selection rules, based on the pulse sequence parameters are derived similar to symmetry based sequences, allowing us to select particular interactions to recouple. In an alternative settings these sequences may also be used for decoupling and along these lines we show that the decoupling performance of EXPORT which is a member of this new family is comparable to the TPPM. To improve the decoupling efficiency further a third modulating field was added (TOFU) which leads to further reduction in resonance line width. Theoretical analysis of EXPORT-CN sequence for first and second order terms is shown and some simulations are presented to discuss the role of homonuclear recoupling in order to facilitate the heteronuclear decoupling. Decoupling experiments are performed to explore the behavior of the EXPORT-CN and TOFU sequences for decoupling and to compare them with TPPM. These experiments show that the oscillating field techniques are capable of decoupling heteronuclear interactions effectively. So using these oscillating field with carefully chosen amplitudes can lead to a better decoupling by systematical suppression of the higher order terms.

This thesis is dedicated to
my lovely brother and sister

Contents

Chapter 1

Introduction

Nuclear Magnetic Resonance (NMR) is a sophisticated and powerful technique which has applications in various disciplines of scientific research and medicine. One of the fields where use of NMR is rapidly increasing is the study of biological system. Solid-state NMR is emerging as an extremely useful tool to study larger bio-molecules. The technique has many advantages as it gives information encoded in anisotropic interactions which averages out in liquids and there is no restriction on size as crystals. Along with the developments in NMR hardware the advancements achieved in pulse designing are playing a key role to make the technique more informative and of wide use. High spectral resolution is obligatory in solid-state nuclear magnetic resonance spectroscopy to study larger biological systems. To get concerning details about the structure one needs to assign the resonances accurately and for that the spectrum should be simple i.e. peaks should be distinguishable and the line width should be as narrow as possible. However, it is still a challenge to get a very high resolution due to presence of the anisotropic interactions and couplings. Heteronuclear decoupling is an important tool to get a less complex and narrow lined high resolution NMR spectra. This improves signal-to-noise ratio by reducing the line width and increasing the peak height. Therefore it is very crucial to have a good decoupling sequence for solids.

1.1 History of decoupling

There are many sequences designed for this purpose both in liquid-state as well as in solid-state NMR. In liquid-state most of the interactions get cancel due to free tumbling motion of the spins so only the isotropic coupling (J- coupling) is the major cause of splitting in spectra. The magnitude of this type of coupling is not very large, it is of the order of hundreds of Hz. The continuous wave (CW) decoupling[1] is one of the oldest sequences to reduce the J coupling. However, if there are many offset resonances then CW is not an efficient decoupling technique. To remedies this, in liquid-state there are multiple-pulse sequences such as WALTZ[2], DIPSI[3] and GARP[4] or by using adiabatic inversion pulses like WURST [5]. Recently, multiple oscillatory fields[6] technique was used to remove the J-coupling. Most of the above mentioned sequences are able to overcome the problem of offset effect as these have

a broadband profile and robustness against RF in homogeneity as well.
In solid-state, we have anisotropic interactions like dipole-dipole coupling interactions (DD) and chemical shift anisotropy (CSA) which are averaged out in case of liquids. These interactions are quite strong compare to J-coupling, one cannot remove them just by using the rf pulses as in the liquids. In 1958 E. Raymond Andrew, A. Bradbury, and R. G. Eades came up with Magic Angle Spinning (MAS) technique[7] which removes the anisotropic interactions up to the first order. This is done by rotating the sample physically around an axis at a specific angle with respect to the main magnetic fields. But at the same time we are introducing one extra time dependency in the Hamiltonian due to this rotation. If we are not using a very high rotor frequency (comparable to the dipolar coupling constant) then the dipolar couplings can not be averaged out by MAS and also there are higher order terms which can not be modulated by this technique. Therefore we have to use additional rf pulses to remove these terms. Removing these unwanted interactions by rf pulses is more effective than by MAS alone even if one uses high rotor frequency (50kHz)[8]. However, its much more difficult to design a good decoupling pulse sequence for the solids than the liquids as there are many different interactions and time dependencies.
Thus the additional time dependencies, large magnitudes of the interactions and presence of both homonuclear and heteronuclear couplings make the decoupling a complicated problem in solid state NMR. There have been a lot of research to get a good decoupling sequence. Initially a strong continuous irradiation CW[1] was used for this purpose. This method is not very effective for fast sample spinning experiments so the first break through to this problem was TPPM[9] by Bennett et al. This was the advent of multiple pulse sequences with modulations in phase, frequency, and/or amplitude for decoupling. There are many derivatives of the TPPM scheme, like FMPM [10] in which frequency modulation is combined with the phase modulation, and AMPM [11]includes amplitude modulation. Fung and co-workers introduced a sequence called SPINAL [12] which involves incremental alteration of the phase of four TPPM units. Another version of TPPM was introduced by Madhu and coworkers [13] which involves an adiabatic sweep of the pulse length in eleven pulse pairs of TPPM. This version of TPPM is called SW_f-TPPM.

1.2 Role of homonuclear coupling and using oscillating fields

Role of homonuclear Coupling to average out the heteronuclear terms has been an issue of debate. People have different opinions about how much the homonuclear coupling is useful in order to remove the higher order $DD \times CSA$ terms. One way of looking at it is that the presence of homonuclear coupling makes the heteronuclear decoupling more complicated [8, 14, 15] because it doesn't commute with similar interaction between other two spins at different times and also not with the heteronuclear coupling so this may result in incomplete averaging of the heteronuclear terms.

On the other hand there are some pulse sequences which exploit the non commuting property of hetero- and homonuclear couplings, as homonuclear coupling is a strong interaction and can be helpful in truncating the heteronuclear interaction[16]. One explanation for the failure of CW at higher spinning frequencies is that at those frequencies the homonuclear couplings are averaged out and CW doesn't recouple those terms so it looses the advantage of truncation.
Simulations, however, do not favor this new approach to decouple using recoupling. The effect of homonuclear coupling on the heteronuclear decoupling in most of the cases seemed to be negative according to the simulations. Nevertheless, it was clear from the simulations that the techniques with the use of oscillating fields, exponentially oscillating fields (EXPORT)[17] and triple oscillating fields (TOFU)[18], can give promising results for decoupling. A similar technique, using continuous phase modulation with constant amplitude [19], was proposed by DePaepe et al in 2003 also has a good decoupling profile.
Since there are experimental evidences that homonuclear recoupling is useful in heteronuclear decoupling as shown by Eden et al[16] and the oscillating field techniques[17] which have good recoupling efficiency, show better decoupling on the simulations, it is worth trying to look for a sequence with good recoupling profile and removing higher order terms so that it can be used for decoupling. Recoupling itself is a very active research topic. There are number of sequences specifically designed to recouple a particular interaction, for dipolar interaction (discussed in chapter-3) Symmetry based pulse sequences[16, 20] are renowned and frequently used. Symmetry based pulses use rotor synchronization to select a particular type of interaction to evolve and the rest are average out. The EXPORT pulse sequence[17] on the other hand has an exponentially oscillating field to recouple homonuclear couplings. In this thesis we present a combination of the two sequences namely EXPORT-CN[21] family of sequences, which gives a better homonuclear recoupling. Then we tried to implement EXPORT-CN for decoupling purpose and it turned out that EXPORT which is a part of this new family of sequences is the best one for decoupling among these sequence. To remove higher order terms and to improve EXPORT we added a third field (Triple Oscillating Field). These sequences give good decoupling performances however there is a room for improvement in their robustness against rf inhomogeneity.

Chapter 2

Basic Theories

Live as if you were to die tomorrow. Learn as if you were to live forever.
– Mahatma Gandhi

In NMR we deal with an ensemble of spins and use quantum statistics to understand the spin dynamics (analytically). We will represent the ensemble by the density matrix and its evolution in time under a Hamiltonian is given by the Liouville-von Neumann equation.

$$\dot{\rho}(t) = -\frac{i}{\hbar}[H, \rho] \tag{2.1}$$

This equation has a simple solution if the Hamiltonian is time independent.

$$\rho(t) = \exp\left(-\frac{i}{\hbar}H(t - t_0)\right)\rho(t_0)\exp\left(\frac{i}{\hbar}H(t - t_0)\right) \tag{2.2}$$

For a time dependent Hamiltonian we use the time dependent Schrodinger's equation for the evolution of the propagator $U(t)$ with time. Then we can write the density matrix at any time t as

$$\rho(t) = U(t, t_0)\rho(t_0)U^{\dagger}(t, t_0) \tag{2.3}$$

and the propagator evolves in time as follows.

$$\frac{d}{dt}U = -iHU \tag{2.4}$$

For analyzing the effect of a pulse sequence on a given system we use some advanced theories as the perturbing (rf) Hamiltonians (and the internal Hamiltonians as well in presence of physical rotation) are time dependent so one has to look for solution of (2.4) with time dependent H.

2.1 Magnus Expansion and Average Hamiltonian Theory

To solve eq.(2.4) for a time dependent Hamiltonian, there are theories like average Hamiltonian theory, perturbation theory, variational method etc. Here without going into details of each of these theories we will use average Hamiltonian theory which is based on Magnus Expansion (ME) [22]. ME gives an approximate solution (or exact but an infinite term series) of a first order matrix differential equation of the form

$$U'(t) = A(t)U(t), \qquad U(0) = I$$

where I is identity matrix. It says that the solution is given by

$$U(t) = \exp(\Omega(t))$$

and $\Omega(t)$ is given by ME as

$$\Omega(t) = \sum_{i=1}^{\infty} \Omega_i(t)$$

where the terms of the series are given by

$$\begin{aligned} \Omega_1(t) &= \int_0^t dt_1 A(t_1) \\ \Omega_2(t) &= \frac{1}{2}\int_0^t dt_1 \int_0^{t_1} dt_2 [A(t_1), A(t_2)] \end{aligned}$$

Here the the brackets denote commutations so one can see that if $A(t)$ commutes with itself at different times (like if A is a constant) then only the first term survives, but if it does not then the situation is complicated and one has to look for convergence of the series and etc. It was Evans[23] and Haeberlen and Waugh who first applied the ME to NMR. To deal with spin dynamics under rf Hamiltonians and to solve the Liouville-von Neumann equation (2.1), Waugh and Haeberlen developed a theory namely Average Hamiltonian Theory (AHT) [24] which makes use of the periodicity and cyclic nature of the Hamiltonians. Since that time, the AHT has been instrumental in the development of improved techniques in NMR spectroscopy. The basic idea of average Hamiltonian theory, for a system governed by $H(t)$, consists of describing the effective evolution within a fixed time interval by an average Hamiltonian $\bar{H}$. The theory states that this is always possible provided $H(t)$ is periodic. The average Hamiltonian depends, however, on the beginning and the end of the time interval observed. It is precisely the average Hamiltonian $\bar{H}$ which is obtained by means of the ME. When the total Hamiltonian splits in a time-independent and a time-dependent piece, $H(t) = H_0 + H_1(t)$, with $H_1(t)$ periodic, an interesting new picture is used, labeled as interaction frame. In this frame the effective Hamiltonian $\tilde{H}(t)$ can be showed[24] as periodic if $H_1(t)$ is periodic in time so that AHT can be applied. So now according to this theory the solution of eq. (2.1) is given by

$$\rho(t) = \exp\left(-\frac{i}{\hbar}\tilde{H}t\right)\rho(0)\exp\left(\frac{i}{\hbar}\tilde{H}t\right)$$

i.e. $U(t) = \exp(-\frac{i}{\hbar}\tilde{H}t)$ where $\tilde{H}$ is the what we get from ME

$$\tilde{H}(t) = \tilde{H}^{(1)} + \tilde{H}^{(2)} + \tilde{H}^{(3)} + \tilde{H}^{(4)}... \quad (2.5)$$

$$\tilde{H}^{(1)} = \frac{1}{\tau_c}\int_0^{\tau_c} dt_1 \tilde{H}(t_1) \quad (2.6)$$

$$\tilde{H}^{(2)} = \frac{1}{2i\tau_c}\int_0^{\tau_c} dt_1 \int_0^{t_1} dt_2 [\tilde{H}(t_1), \tilde{H}(t_2)] \quad (2.7)$$

2.2 BCH expansion and Semi-continuous BCH Theory

The Baker-Campbell-Hausdorff theorem expresses the product of exponentials of matrices in exponential of a summation series. This theorem can be derived from the ME as well by considering the operator (here Hamiltonian) piecewise constant. In such cases one can replace the integrals by summations over the interval of constant behavior of the Hamiltonian then Magnus Expansion leads us to the well known BCH expansion[**?**].

$$H(t) = H^{(1)} + H^{(2)} + H^{(3)} + H^{(4)}... \quad (2.8)$$

$$H^{(1)} = \frac{1}{\tau_c}\sum_1^n \tau_i H_i \quad (2.9)$$

$$H^{(2)} = \frac{1}{2i\tau_c}\sum_{i>j}^n \tau_i\tau_j [H_i, H_j] \quad (2.10)$$

semi-continuous BCH formula is basically a combination of the ME and the BCH expansion. It is very useful in NMR calculations as there we often deal with Hamiltonians which change the profile suddenly. For example in multiple pulse sequence experiments where the phase and the amplitude of the rf Hamiltonian changes abruptly at the end of one pulse and the beginning of another. In such conditions it becomes very difficult to get the higher order terms of ME as the calculation of integrals over the whole period become very lengthy. This can be remedies if we can approximate the Hamiltonian as a constant for a short time then the BCH can be exploited, the trick is that we use ME to get the average Hamiltonian for short time periods and then use this hamiltonian as a constant for that time period to make use of the BCH expansion [25] for the whole sequence. Thus the semi continuous BCH expansion is given by

$$H_i(t) = H_i^{(1)} + H_i^{(2)} + H_i^{(3)} + H_i^{(4)}... \quad (2.11)$$

$$H^{(1)} = \frac{1}{\tau_c}\sum_1^n \tau_i H_i^{(1)} \quad (2.12)$$

$$H^{(2)} = \frac{1}{\tau_c}\sum_1^n \tau_i H_i^{(2)} + \frac{1}{2i\tau_c}\sum_{i>j}^n \tau_i\tau_j[H_i^{(1)}, H_i^{(1)}] \quad (2.13)$$

$$(2.14)$$

Here the subscripts $i, j, k...$ represent the intervals of constant Hamiltonian and in each interval we use ME to get all orders of H_i. We will use this approach to analyze the symmetry based pulse sequences and the new EXPORT-CN sequences. So far we have discussed the useful theories to get the evolution of the spin system yet we did not talk about the representation of all the Hamiltonians and density matrices. To understand the dynamics analytically, the spin system i.e the density matrix and the Hamiltonian can be written either in form of product operators or second rank tensors.

2.3 Product Operator Formulism

Hamiltonian for a spin with angular momentum $\mathbf{I}$ under an external field $\mathbf{B}$ is given by $H = -\mu.\mathbf{B}$ where $\mu = \gamma\mathbf{I}$. We can take the magnetic field along z-axis with magnitude B_0 so the Hamiltonian is $H = -\gamma I_z B_0 = \omega_0 I_z$ here $\omega_0 = -\gamma B_0$ is known as the Larmor frequency. Similarly the rf Hamiltonian can also be written as $H_{rf} = \omega_{rf} I_\phi$ here ϕ is the phase of the rf pulse such that $I_\phi = I_x\cos(\phi) + I_y\sin(\phi)$. Every interaction Hamiltonian can be represented in terms of these product operators (I_x, I_y, I_z). For more than one spin, there are coupling Hamiltonians which are outer products of the operators. For example scaler coupling Hamiltonian for a two spin system is given by $H_J = 2\pi J\mathbf{I}\bigotimes\mathbf{S}$ or if we write all the operators as 4×4 by taking outer products with identity matrix i.e.I_x as $I_x\bigotimes I$ and S_x as $S\bigotimes S_x$ and so on, then $H_J = 2\pi J\mathbf{I}.\mathbf{S}$ where dot is simple matrix product and J is coupling constant. Thus every Hamiltonian can be expressed in this formulism. The evolution of density matrix (2.2), under any Hamiltonian, can be simplified using a formula.

$$\exp(-i\phi B)A\exp(i\phi B) = A\cos(\phi) + i[A,B]\sin(\phi) = A\cos(\phi) - iC\sin(\phi) \quad (2.15)$$

But this is true only if A, B and C are cyclically commuting i.e

$$[A,B] = iC,\ [B,C] = iA,\ \text{and}\ [C,A] = iB$$

This condition is satisfied by the product operators therefore (2.15) is very useful in all the analytical calculations of NMR in this formulism.

2.4 Tensor Representation and Wigner's Rotations

Another way doing all the calculations is using a tensorial representation. Every Hamiltonian can be written as dot product of two tensors namely space and spin tensors. Further one can express those in terms of irreducible spherical tensors in this framework we use Wigner matrices to rotate a tensor under the effect of a Hamiltonian. The Hamiltonian has following form with $m = -l \dots l$ and $\mu = -\lambda \dots \lambda$ for a given interaction Λ.

$$H^{\Lambda}_{l,m,\lambda,\mu} = A^{\Lambda}_{l,m} T^{\Lambda}_{\lambda,\mu} \tag{2.16}$$

Here $A_{l,m}$ is the space part and $T_{\lambda,\mu}$ is the spin part so all the physical rotations will affect the first part of the Hamiltonian and the rf pulses will show there effect by modifying the second part of it. To transform from one frame to another we use Wigner's matrices[26], if Ω is set of Euler angles (α, β, γ) which relates any tensor $T_{\lambda,\mu}$ from on frame to a new rotated frame where it is given by $T'_{\lambda,\mu}$ then the two tensors are related by following equation.

$$T'_{\lambda,\mu} = \sum_{\mu'} T_{\lambda,\mu'} D^{\lambda}_{\mu',\mu}(\Omega) \tag{2.17}$$

If there are multiple transformations then we can write simply by cascading the Wigner Matrices. This makes it very easy to handle many frame transformations.

$$T''_{\lambda,\mu} = \sum_{\mu'\mu''} T_{\lambda,\mu''} D^{\lambda}_{\mu'',\mu'}(\Omega_2) D^{\lambda}_{\mu',\mu}(\Omega_1) \tag{2.18}$$

$T''_{\lambda,\mu}$ is the new tensor after two rotations. Wigner matrices, D, can be reduced to an irreducible form d by writing

$$D^{\lambda}_{\mu',\mu}(\alpha, \beta, \gamma) = e^{-i\mu'\alpha} d^{\lambda}_{\mu',\mu}(\beta) e^{-i\mu\gamma} \tag{2.19}$$

In NMR we generally do all the calculations in the laboratory frame (lab frame) so one has to transform from the principal axis frame to the lab frame this is done by multiple transformations consecutively to visualize all the transformations see fig.2.1. All these frame are related only by physical rotations i.e. there is no effect on the spin part of an interaction and the spatial part can be written as

$$(A_{l,m})^L = \sum_{m''',m'',m'} (A_{l,m'''})^P D^{l}_{m''',m''}(\Omega_{PM}) D^{l}_{m'',m'}(\Omega_{MR}) D^{l}_{m',m}(\Omega_{RL}) \tag{2.20}$$

$$(A_{l,m'})^R = \sum_{m''',m''} (A_{l,m'''})^P D^{l}_{m''',m''}(\Omega_{PM}) D^{l}_{m'',m'}(\Omega_{MR}) \tag{2.21}$$

$$(A_{l,m})^L = \sum_{m'} (A_{l,m'})^R e^{(-im'(\alpha^0_{RL} - \omega_r t))} d^{l}_{m',m}(\beta_{RL}) \tag{2.22}$$

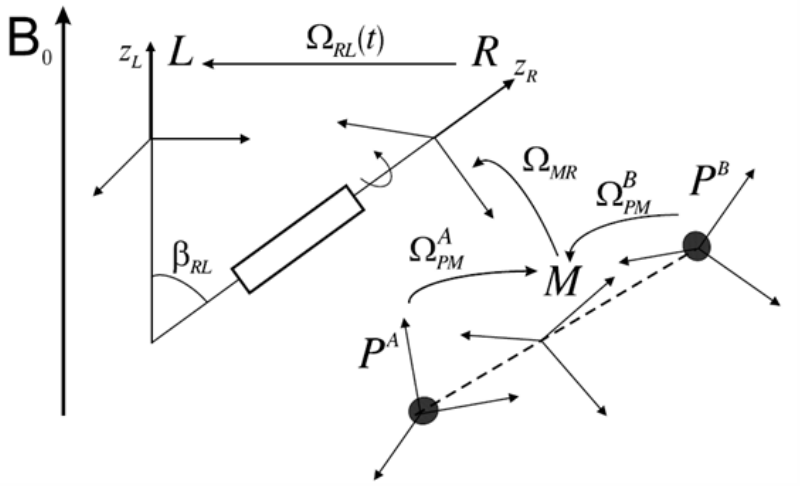

Figure 2.1: *Visualization of different frames and transformations from the principal axis frame to the laboratory frame.* P^A *and* P^B *are the principal axis frames,* M *is the molecular frame,* R *is the rotor frame and* L *represents the Lab frame* Ω *are the angles relating these frames with each other. This figure is adopted directly from Mattias Eden's PhD thesis*

Here the last transformation (Rotor frame to Lab frame) is shown separately as it is important due to the introduction of a time dependency through rotor frequency (ω_r). In the next chapters we will write the spatial part in fourier series where this frequency is important.

Chapter 3

Homonuclear Recoupling

When you do nothing, you feel overwhelmed and powerless. But when you get involved, you feel the sense of hope and accomplishment that comes from knowing you are working to make things better.

The use of MAS to average out the anisotropic interactions to the first order promotes the high-resolution spectra in the detection dimension but it entails use of recoupling techniques to reintroduce the anisotropic interactions selectively. These interactions are necessary to mediate coherence/polarization transfer and to obtain information about the structure and the dynamics(e.g. the internuclear distances and the torsion angles). Therefore the recoupling techniques are of fundamental importance in the ssNMR and there are many experiments designed for this purpose. Most of such sequences rely on the concept of interference between the rotor frequency and the modulations cause by rf fields. But many of the sequences so far suffer from the problems like dipolar truncation and sample heating due to high power irradiation. The dipolar truncation is a phenomenon according to which if there is a network of three or more spins, coupled to each other with different coupling strengths then the stronger couplings cause truncation in the weaker couplings due to the non commuting nature of the coupling Hamiltonians. This causes loss of the information which one gets from the long distant coupled nuclei as they are weakly coupled. The second difficulty was the heating of the sample as we need to decouple the protons while recoupling other nuclei and this needs high power irradiation on the proton channel which causes extra heating. Both the problems have been addressed by several groups and some solutions have been proposed. To get rid of the dipolar truncation people use sparsely labeled sample rather than uniformly labeled so that one get information from weak couplings in the absence of strong couplings. Another approach is to modify the coupling Hamiltonian such that only the commuting Ising part of it survives, this can be done using pulse engineering. The coupling Hamiltonian is of the form $2I_zS_z - I_xS_x - I_yS_y$ where the first part (secular part) is known as the Ising operator, which commutes with the Ising operator of different spin pairs so no risk of truncation. The Triple oscillating field (TOFU) sequence [18]is designed by group of Khaneja and Nielsen to prepare such Hamiltonians it recouples only the isotropic Chemical Shift and removes the CSA so that in the coupling Hamiltonian only the Ising part remains. This sequence was

modified further with addition of fourth field (FOLD)[27].
To deal with the heating problem, sequences with low power requirement are needed to be developed. Exponentially oscillating fields (EXPORT) [17] is a sequence which recouples without irradiating the protons as it takes care of decoupling intrinsically. It uses a small exponentially oscillating field in addition to a relatively large continuous field. This small field is chosen such that in the frame of the large field it meets the HORROR condition and cause recoupling (discussed below in detail). The EXPORT-CN sequence is further advancement of the EXPORT sequence in which we merge the EXPORT and the CN symmetry sequences. To analyze this new sequence first we will briefly look at the theory of the EXPORT and the symmetry based pulses.

3.1 EXPORT

The Hamiltonian for the EXPORT is given by following equation.

$$H^{rf}(t) = C_I I_x + C_S S_x + B_I e^{-iC_I I_x t} I_z e^{iC_I I_x t} + B_S e^{-iC_S S_x t} S_z e^{iC_S S_x t} \tag{3.1}$$

Here the coefficients Cs and Bs were chosen according to the purpose. Generally C is a strong field ($6\omega_r$) compare to B. To implement this on the spectrometer a rf field of magnitude

$$A_k = \sqrt{C_k^2 + B_k^2 \cos^2(C_k t)}$$

and phase

$$\arctan\left(\frac{B_k \cos(C_k t)}{C_k}\right) + \frac{B_k}{C_k}(\cos(C_k t) - 1)$$

can be used to produce the same field as (3.1). The recoupling is decided by the difference of the modulating fields on the two channels $B_I - B_S$. To see the effect on the heteronuclear coupling we will transform the coupling Hamiltonian to the frame of rf for that we will do consecutive frame transformations, first we will go to the frame of main rf field i.e. C-frame and then to the frame of modulating field i.e. B-frame.

$$\begin{aligned} H_{IS} &= 2I_z S_z - I_x S_x - I_y S_y \\ \tilde{H}_{IS} &= \frac{1}{2}(I_z S_z + I_y S_y) - I_x S_x \end{aligned} \tag{3.2}$$

Rest of the terms are modulated with a frequency C or $2C$ assuming that C is very high compare to B and ω_r we can ignore those terms. So in B-frame we will have

$$\tilde{\tilde{H}}_{IS} = \frac{1}{2} I_z S_z + \frac{1}{2} I_y S_y [\cos(B_I - B_S)t + \cos(B_I + B_S)t]... \tag{3.3}$$

If $B_I - B_S = n\omega_r$ then it recouples the heteronuclear couplings by producing static terms due to interference with the rotor frequency. The robustness against inhomogeneity was ensured by switching the sign of C in each loop[17] so that the effect of the inhomogeneity is refocused. Now the other important component of the new sequence is a CN symmetry sequence. There are two families of symmetry based pulse sequences namely CN and RN symmetries. In the next section we will discuss the theory of these pulses and derive the selection rules.

3.2 Symmetry based pulses

Now when we are equipped with the tools like the Wigner rotations and the average Hamiltonian theory, it is time to analyze these advanced pulse sequences. To see the effect of a rf pulse we will simply change our frame of reference to the rf frame using the Wigner matrices and the tensor form of internal Hamiltonian. But before going to the mathematical analysis it would be advantageous to have a look on the structure of these pulses and to have an intuitive idea about how these work. Mainly there are two classes of symmetry namely C and R, then one can further classify them by combining with the different methods of super cycling i.e. SM^{χ} and $SM^{\chi}SM^{-\chi}$. But we will restrict ourself to the discussion of these two classes, especially the C symmetries as these are important in present work. These two classes are different mainly in the basic element and then slightly differ in the pattern of phase changing. Every sequence can be defined using three symmetry numbers denoted as N, n, and ν. N is the number of cyclic pulses with different phases, n is the number of rotor periods a pulse sequence span for and ν sets the change in phase after each cyclic pulse, the phase shift is given by $2\pi\nu/N$ for C sequences and $\pi\nu/N$ for R sequences. So one can look at these numbers as if n is the spatial winding number and ν is the spin winding number. We have a basic element which is a 2π or its integer multiple (including zero) rotation for the C sequences and for the R sequences a π rotation followed by another π rotation with a 180^0 phase addition. We apply this element N times in n rotor periods each time we shift its phase by a factor given above. It is clear that we have a relation in rotor frequency and rf frequency (as n rotor periods are being completed in N full rotations by rf fields) which causes a connection in physical rotation due to rotor and spin rotation due to pulses. The way of changing phases of consecutive π or 2π pulses is such that for some selected terms these two rotations interfere destructively and result in no net oscillation causing refocusing of these terms and the rest all get averaged due to the modulations. As spatial and spin rotations depend on indices m and μ, we have selection rules depending on m, μ and N, n, ν. Mathematically one can derive the selection rules and the expressions for the scaling factors using the average Hamiltonian theory and the semi BCH expansion. This looks difficult to analyze as there are many pulses with different phases but the phase change occurs in a very systematic way and it occurs after a full rotation so one can make use of this symmetry to do the calculations in a simpler fashion. We can write the Hamiltonian as a sum of all the different interaction Hamiltonians.

$$H(t) = H_{rf}(t) + \sum_{\Lambda m} H^{\Lambda}_{lm\lambda 0}(t) \tag{3.4}$$

Here Λ represents the interaction, it may be Zeeman, DD, CSA, or J. Note that we have put $\mu = 0$ in the beginning due to secular approximation (as rest of the terms are negligible and they don't commute with Zeeman interaction). The values of l and λ may change with different interactions (i.e. different Λ) depending on the rank of the spin and the space tensors for that particular interaction, so the summation over Λ implies a summation over all possible values of l and λ. The

Hamiltonian in the Lab frame can be written in following way using (2.20).

$$H^{\Lambda}_{lm\lambda 0} = \omega^{\Lambda}_{lm}(t) T^{\Lambda}_{\lambda 0} \tag{3.5}$$

We can write $\omega^{\Lambda}_{lm}(t)$ as a fourier series

$$\begin{aligned} \omega^{\Lambda}_{lm}(t) &= \omega^{\Lambda}_{lm} e^{im\omega_r t} \\ \text{where } \omega^{\Lambda}_{lm} &= [A^{\Lambda}_{lm}]^R e^{-im\alpha^0_{RL}} d^l_{m0}(\beta_{RL}) \end{aligned} \tag{3.6}$$

This whole Hamiltonian can be transformed into the frame of rf to analyze the effect of the pulse sequence. In this thesis we will take a C symmetry to explain this (we will use C symmetry in the new pulse sequence also). Consider $(q+1)^{th}$ rf cycle i.e. after q no. of 2π pulses with different phases during $(q+1)^{th}$ pulse such that the time is $t_q = t^0_q + t = q\tau + t$, the phase is $\phi = \gamma_0 + 2\pi q\nu/N$, γ_0 being the initial phase and rotation due to rf pulse is $\beta = \omega_{rf}(q\tau + t) = \omega_{rf} t$. Therefore we have the Euler angles as $\Omega = (\phi, \beta, 0)$ to go to the frame of rf. So the internal Hamiltonian in the rf frame at time t_q ($\tilde{H}(t_q)$ tilde represents a frame transformation) can be written as

$$\tilde{H}(t_q) = \sum_{\Lambda m\mu} \tilde{H}^{\Lambda}_{lm\lambda\mu}(t_q) = \sum_{\Lambda m\mu} \tilde{\omega}^{\Lambda}_{lm}(t_q) \tilde{T}^{\Lambda}_{\lambda\mu}$$

The rf pulses affect only the spin part which can be taken into account using the Wigner rotations and the spatial part remain as it is, we will just put this in the fourier form.

$$\tilde{H}^{\Lambda}_{lm\lambda\mu}(t_q) = \omega^{\Lambda}_{lm} e^{im\omega_r t_q} T^{\Lambda}_{\lambda\mu} e^{-i\mu(\gamma_0 + \frac{2\pi\nu q}{N})} d^{\lambda}_{\mu,0}(-\beta) \tag{3.7}$$

This can be further simplified by putting the value of β and using the relation between τ and τ_r (i.e $N\tau = n\tau_r$).

$$\tilde{H}^{\Lambda}_{lm\lambda\mu}(t_q) = \omega^{\Lambda}_{lm} e^{i(m\omega_r t + \mu\gamma_0)} T^{\Lambda}_{\lambda\mu} e^{i\frac{2\pi(mn-\mu\nu)q}{N}} d^{\lambda}_{\mu,0}(-\omega_{rf} t) \tag{3.8}$$

To make the expression simpler lets define $mn - \mu\nu = M$ and for further calculations we will use a shorthand notation for an integral as defined below.

$$\Gamma_{lm\lambda\mu} = \int_0^{\tau_c} dt \omega^{\Lambda}_{lm} e^{i(\mu\gamma_0)} d^{\lambda}_{\mu,0}(\omega_{rf} t) \tag{3.9}$$

The first order Hamiltonian for $(q+1)^{th}$ cycle for any given interaction (Λ) in the frame of rf can now be calculated using the AHT (2.5).

$$\bar{\tilde{H}}^{\Lambda(1)}_{lm\lambda\mu} = \frac{1}{\tau_c} \Gamma_{lm\lambda\mu} e^{i\frac{2\pi M q}{N}} T^{\Lambda}_{\lambda\mu} \tag{3.10}$$

This is the average Hamiltonian for one interaction in one rf cycle, to get complete Hamiltonian in one cycle we should take a summation over Λ. To keep it neat we will do the first order calculations for one interaction in case of second order we will need at least two interactions at a time. If we take it for entire pulse sequence then

we can use semi BCH theory (2.11). This gives the average Hamiltonian for a given interaction over the whole pulse sequence i.e. N cycles.

$$\bar{\tilde{H}}^{\Lambda(1)}_{lm\lambda\mu} = \frac{1}{N\tau_c}\sum_{q=0}^{N-1}\Gamma_{lm\lambda\mu}e^{i\frac{2\pi Mq}{N}}T^{\Lambda}_{\lambda\mu} \tag{3.11}$$

By defining

$$S_{lm\lambda\mu} = \frac{1}{N}\sum_{q=0}^{N-1}e^{i\frac{2\pi Mq}{N}}$$

it can be seen that

$$S_{lm\lambda\mu} = \begin{cases} 1 & \text{if } M = Nz \\ 0 & \text{if } M \neq Nz \end{cases}$$

Therefore the first order Hamiltonian (3.13) is zero if

$$mn - \mu\nu \neq Nz. \tag{3.12}$$

Another way of getting the expression for the scaling factor without going into this much analytical work is given by Matias Eden and M.H. Levitt [16]. In this approach they used the fact that this Hamiltonian is periodic in time with period $N\tau$ this way it is easier to get the second order selection rules as well but this approach does not tell anything about the scaling factor. After getting the selection rule now we want to have the expression for the scaling factor which gives us the measure of the effect of a symmetrically allowed term. So the scaling factor is basically the magnitude of contribution from a particular allowed term. For this eq. (3.11) can be rewritten by using eqs (3.9)(3.5)(3.6).

$$\bar{\tilde{H}}^{\Lambda(1)}_{lm\lambda\mu} = \frac{1}{N\tau_c}S_{lm\lambda\mu}\Gamma_{lm\lambda\mu}T^{\Lambda}_{\lambda\mu} \tag{3.13}$$

$$\bar{\tilde{H}}^{\Lambda(1)}_{lm\lambda\mu} = \frac{1}{N\tau_c}S_{lm\lambda\mu}k_{lm\lambda\mu}T^{\Lambda}_{\lambda\mu}[A^{\Lambda}_{lm}]^R \tag{3.14}$$

The scaling factor is given by $k_{lm\lambda\mu}$ as

$$k_{lm\lambda\mu} = \frac{1}{\tau_c}\int_0^{\tau_c} dt e^{-i(m\alpha^0_{RL} - m\omega_r t - \mu\gamma_0)}d^l_{m0}(\beta_{RL})d^{\lambda}_{\mu,0}(\omega_{rf}t) \tag{3.15}$$

By choosing a particular sequence one can select allowed terms and cancel others but the contribution from any selected term can not be controlled by this. Sometimes it is possible that a term is allowed symmetrically but its scaling factor is zero so there is no effect of that interaction. In the next section we will discuss about the newly developed EXPORT-CN sequences in which one can control the scaling factor by changing the value of an applied oscillating field.

3.3 EXPORT-CN Sequence

We saw that the EXPORT is a low power recoupling technique and the symmetry based sequences are general recoupling sequences which allow us to choose a particular interaction to recouple. The limitation of the symmetry sequences is that

one has no control over the scaling factor of a symmetrically allowed term i.e. these sequences provide a great selectivity but the magnitude of these selective terms can be very less (even zero). Here is an attempt to govern the scaling factor to some extent. This is done by combining the EXPORT and the CN sequences by replacing the large continuous field in the EXPORT scheme by a suitable symmetry. This way we have same selectivity of the terms but now we have a scaling factor dependent of the small field. The theory is similar to the CN sequences, here also we will use the average hamiltonian theory the only change is that now we have one more rotation. The effect of this extra rotation is that now we have slightly modified selection rules and an additional factor in scaling factor expression which enables us to have a control over scaling factor. The rf Hamiltonian for the EXPORT-CN[21] sequence is given by

$$H^{rf}(t) = CI_{\phi} + Be^{-iCI_{\phi}t}I_z e^{iCI_{\phi}t} \tag{3.16}$$

So in the frame of the large rf field (i.e symmetry based pulse) the internal Hamiltonian takes the form shown as in eq. (3.8) and the rf Hamiltonian is

$$\tilde{H}^{rf} = BI_z \tag{3.17}$$

Further going to frame of this rf Hamiltonian we can write the internal Hamiltonian just by doing one more z-rotation. Here it is quite simple to include this rotation as it is a z-rotation. It will cause only an extra phase in the Hamiltonian we had in CN frame.

$$\tilde{\tilde{H}}^{\Lambda}_{lm\lambda\mu}(t_q) = \omega^{\Lambda}_{lm}e^{i(m\omega_r t+\mu\gamma_0)}T^{\Lambda}_{\lambda\mu}e^{i\frac{2\pi(mn-\mu\nu)q}{N}}d^{\lambda}_{\mu,0}(-\omega_{rf}t)e^{i\mu Bt_q}$$

which can be written in a convenient form as

$$\tilde{\tilde{H}}^{\Lambda}_{lm\lambda\mu}(t_q) = \omega^{\Lambda}_{lm}T^{\Lambda}_{\lambda\mu}e^{i(\mu(\gamma_0-Bt))}d^{\lambda}_{\mu,0}(-\omega_{rf}t)e^{i\frac{2\pi(mn-\mu\nu-\mu n\frac{B}{\omega_r})q}{N}} \tag{3.18}$$

In the analogy with eq (3.10) the first order Hamiltonian now can be written in a simple form by defining $mn-\mu\nu-\mu n\frac{B}{\omega_r} = M_B$ and the integral

$$\Gamma^{B}_{lm\lambda\mu} = \int_0^{\tau_c} dt\omega^{\Lambda}_{lm}e^{i(\mu\gamma_0-Bt)}d^{\lambda}_{\mu,0}(\omega_{rf}t) \tag{3.19}$$

So that the first order Hamiltonian can be given as

$$\bar{\bar{\tilde{H}}}^{\Lambda(1)}_{lm\lambda 0} = \frac{1}{\tau_c}\Gamma^{B}_{lm\lambda\mu}e^{i\frac{2\pi M_B q}{N}}T^{\Lambda}_{\lambda\mu} \tag{3.20}$$

The full first order Hamiltonian will give slightly modified selection rules given by

$$mn-\mu\nu-\mu n\frac{B}{\omega_r} \neq Nz \tag{3.21}$$

here it should be noted that $n\frac{B}{\omega_r}$ is an integer and the scaling factor now is

$$k^{B}_{lm\lambda\mu} = \frac{1}{\tau_c}\int_0^{\tau_c} dt\omega^{\Lambda}_{lm}e^{i(\omega_r(m-\mu\frac{B}{\omega_r})t+\mu\gamma_0)}d_{\mu,0}(\omega_{rf}t) \tag{3.22}$$

Table 3.1: *Scaling factors of homonuclear coupling terms under* $C6_4^1$ *and* $C6_4^1$+$EXP(B = -1/4)$

term	$C6_4^1$	$C6_4^1 + EXP(B = -1/4)$
2,-2,2,-2	0.0465	0.0676
2,1,2,-2	0.0822	0.1503

Using these expressions in MATHEMATICA to calculate the scaling factor for the allowed terms we found that the sequences $C6_4^1 + EXP(B = -1/4)$ and $C6_4^1$ allow same terms i.e these two have exactly same selection rules. But there is a increment in the scaling factors of homonuclear coupling terms 3.1. This illustrates the advantage of this extra small oscillating field. Now the question is to choose appropriate value of B. However we have a restriction over B that $n\frac{B}{\omega_r}$ have to be an integer yet just to get an idea about the effect of B on the scaling factor for a given symmetry, the value of scaling factors were plotted against different B-values **??**. It is clear from the plot that gain is maximum for B near $-\frac{1}{2}$ or $-\frac{1}{2}$. We took $B = -\frac{1}{4}$ as our target terms were the ones allowed by symmetry $C6_4^1$ so to match the selection rules ($B = -\frac{1}{4}$ and $n = 4$) were the parameter values suited. The symmetries $C3_2^1$ and $C6_4^2$ are same but in former nB is not an integer so we chose the later one.

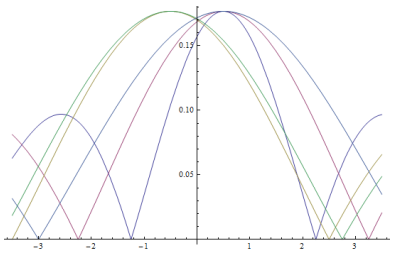

Figure 3.1: *The different colors are for different CN sequences on the y-axis the values are of scaling factors for allowed homonuclear coupling terms and on the x-axis the small field B. Global maxima are either at* $\frac{1}{2}$ *or at* $-\frac{1}{2}$ *depending on the allowed term it is observed that if the product* $(m\mu)$ *is positive then the maxima is at negative B and vice versa*

3.4 Simulations and Experimental Results

The overall pulse scheme for 2D MAS NMR $^{13}C, ^{13}C$ chemical shift correlation is shown in figure 3.2. The amplitude and phase profiles of the three pulses which were used in all the experiments and simulations are also shown (c-e). The last part of the figure is visualization of how the overall phases and amplitudes are changing with time when these are used as a basic elements of a CN symmetry. All the simulations for different recoupling sequences were carried out on SIMPSON and SIMMOL was used to obtain the typical chemical shifts and dipolar couplings. Powder averaging, with 5 γ_{PR} angles and crystal file rep144 i.e. 144 $\alpha_{PR,\beta_{PR}}$ REPULSION angles, was used. The efficiencies of $^{13}C_\alpha$ to $^{13}C_\beta$ coherence transfers were compared for three different mixing sequences ($C3_1^1\bar{C}3_1^1, C3_2^2\bar{C}3_2^2$ and EXPORT-$C6_4^2$ with

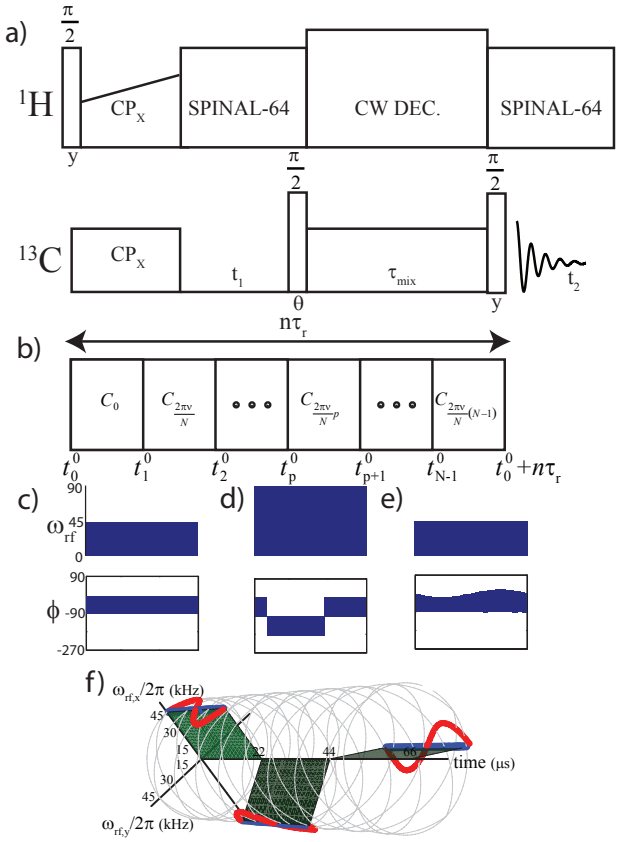

Figure 3.2: *(a)Pulse sequence for 2D MAS NMR* $^{13}C, ^{13}C$ *chemical shift correlation using symmetry based pulse sequences during the mixing part of the sequence. (b)blocks of a CN sequence. (c-e)different basic elements used in CN sequences with specific rf strength(kHz, on the vertical axis) and phases in degrees: (c) standard* $2\pi_x$*element (d) POST* $\pi/2_x 2\pi_{-y} 3\pi/2_x$ *element (e) EXPORT element using* $C = 3\omega_r/2$ *and* $B = -\omega_r/4$*. (f)Rf field trajectories: blue lines show the rf field as function of time for CN sequence with the basic element* $2\pi_x$ *and red lines are for the EXPORT-CN sequence i.e. EXPORT is used as the basic element.*

$C = 3\omega_r/2, B = -\omega_r/2$). In figure 3.3 (a) and (b) correspond to coherence transfer versus mixing time at 16.4T, (a)is comparison of POST-$C3_2^2\bar{C}3_2^2$ ($\pi/2_x 2\pi_{-y} 3\pi/2_x$ elements) shown in blue and $C3_1^1\bar{C}3_1^1$ ($2\pi_x$ element) in red, assuming $10kHz$ spinning frequency and $30kHz$ rf power. In (b) the spinning frequency is $30.3kHz$ and rf power approximately $45kHz$, the blue is for $C3_1^1\bar{C}3_1^1$ ($2\pi_x$ element) and the red one corresponds to EXPORT-$C6_4^2$ with $C = 3\omega_r/2, B = -\omega_r/2$. These simulations show that low-power phase-alternated symmetry based sequences are capable of mediating efficient coherence transfer and the mixing times, $2.0ms$ for POST-$C3_2^2\bar{C}3_2^2$ and $1.2ms$ for $C3_1^1\bar{C}3_1^1$, indicate the difference in the scaling factors.
Under high spinning conditions the maximum transfer, in case of EXPORT-$C6_4^2$, exceeds 70 with very fast building up in $1.12ms$ as compare to $1.98ms$ for $C3_1^1\bar{C}3_1^1$. Sub-figures (c to f) in the same figure provide 2D offset profile for these sequences : (c)POST-$C3_2^2\bar{C}3_2^2$ ($\pi/2_x 2\pi_{-y} 3\pi/2_x$ elements) (d)$C3_2^2\bar{C}3_2^2$ ($2\pi_x$ elements) (e)$C3_1^1\bar{C}3_1^1$ ($2\pi_x$ elements) and (f)EXPORT-$C6_4^2$ with $C = 3\omega_r/2, B = -\omega_r/2$ the spinning frequency for (c) and (e) was taken to be $10kHz$ and for (d) and (f) it was $30.3kHz$. It is observed that all the sequences provide the efficient transfer over the full aliphatic region the EXPORT-CN sequence has the highest efficiency. The experiments were carried out on wide bore Bruker Avance 400MHz (9.4T) spectrometer with standard triple resonance $2.5mm$ solid-state probe. The sample, alanine (α, β labeled), was purchased from Isotech. Inc. (Miamisburg, OH). To verify the simulation results the coherence transfer efficiencies of the three sequences ($C3_1^1\bar{C}3_1^1, C3_2^2\bar{C}3_2^2$ and EXPORT-$C6_4^2$ with $C = 3\omega_r/2, B = -\omega_r/2$) were demonstrated (comparing the peak intensities for $^{13}C_\beta$ relative to the initial $^{13}C_\alpha$ state). The transfer around 50% was shown by POST-$C3_2^2\bar{C}3_2^2$ ($\pi/2_x 2\pi_{-y} 3\pi/2_x$ elements) and $C3_1^1\bar{C}3_1^1$ ($2\pi_x$ elements) at a spinning frequency of $10kHz$ while the $C3_2^2\bar{C}3_2^2$ ($2\pi_x$ elements) at $30.3kHz$ spinning frequency transferred 62.5% a little lesser compare to EXPORT-$C6_4^2$ 67.8% at the same spinning. The mixing times are very similar to the numerical predictions. Figures (c) and (d) show the experimental rf mismatch curves for the four experiments

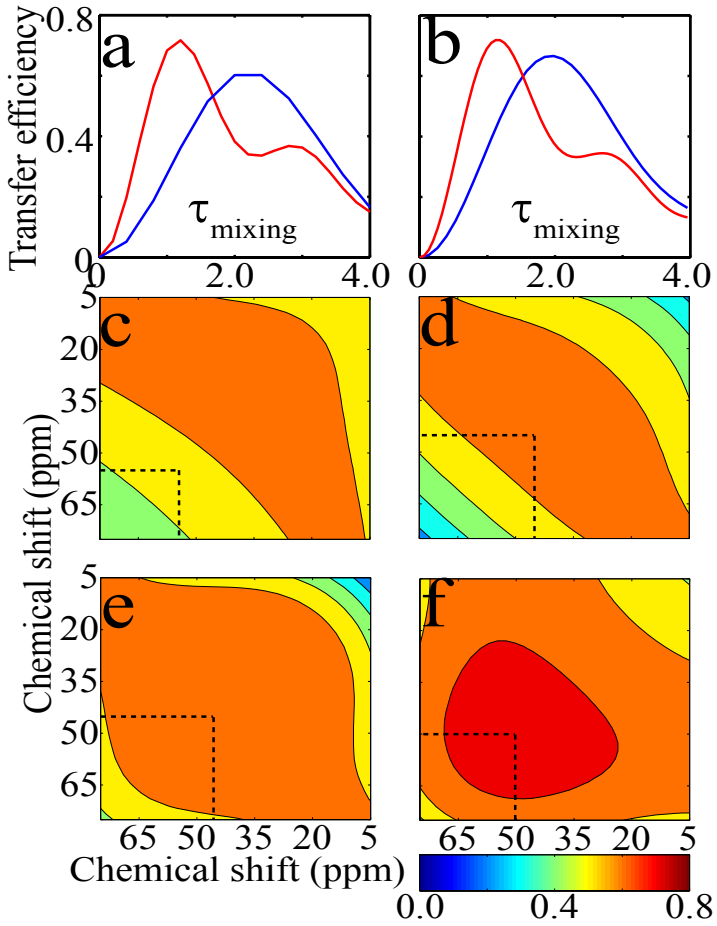

Figure 3.3: *Numerical simulations of the efficiency of* $^{13}C_\alpha$ *to* $^{13}C_\beta$ *coherence transfer between typical aliphatic (e.g.,* $^{13}C_\alpha$ *and* $^{13}C_\beta$ *in an amino acid residue) as function of excitation time (a,b) and 2D offset variation (c-f). All simulations assume a magnetic field of 16.4 T, spin system parameters (except isotropic chemical shifts) corresponding to the* $^{13}C_\alpha - {}^{13}C_\beta$ *spin pair of L-alanine , and initial spin-operator being* I_z *on* $^{13}C_\alpha$ *and the detection operator being* S_z *on* $^{13}C_\beta$ *. Recoupling sequence, rf field strength, spinning speed parameters for the simulations (a)* $10kHz$ *spinning,* ^{13}C *rf field strength of* $30kHz$ *corresponding to POST-*$C3_2^2\bar{C}3_2^2$ *(*$\pi/2_x 2\pi_{-y} 3\pi/2_x$ *elements) in blue and* $C3_1^1\bar{C}3_1^1$ *(*$2\pi_x$ *elements) in red. (b)* $30.3kHz$ *spinning,* ^{13C} *rf field strength of* $45kHz$ *corresponding to* $C3_2^2\bar{C}3_2^2$ *(*$2\pi_x$ *elements) in blue and EXPORT-*$C6_4^2$ *(*$C = 3\omega_r/2, B = -\omega_r/2$*) in red. (c-f) Offset profiles for the POST-*$C3_2^2\bar{C}3_2^2$ *(*$\pi/2_x 2\pi_{-y} 3\pi/2_x$ *elements) (c) and* $C3_1^1\bar{C}3_1^1$ *(*$2\pi_x$ *elements) (e) using* $10kHz$ *spinning and* $C3_2^2\bar{C}3_2^2$ *(*$2\pi_x$ *elements) (d) and EXPORT-*$C6_4^2$ *(*$C = 3\omega_r/2, B = -\omega_r/2$*)(f) using* $30.3kHz$ *spinning.*

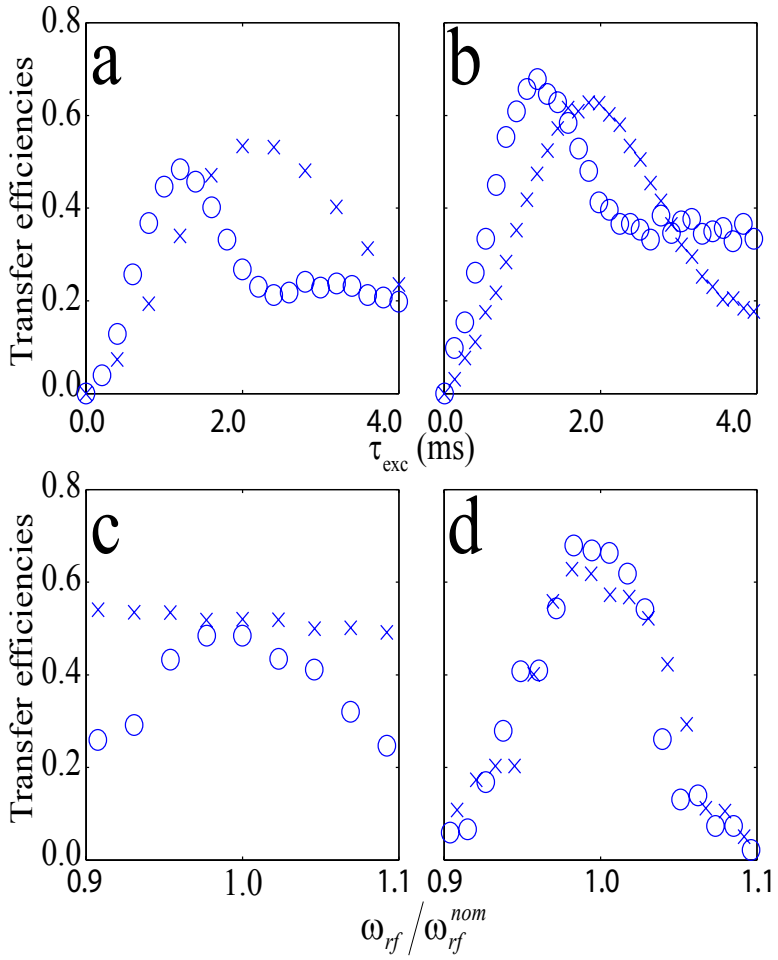

Figure 3.4: *Experimental demonstration of the efficiency of* $^{13}C_\alpha$ *to* $^{13}C_\beta$ *polarization transfer obtained for* $2,3-{}^{13}C_2-L$*-alanine at* $9.4T$ *as function of (a,b) the mixing time and (c,d) rf mismatch (ratio between actual and nominal rf field strength) using (a,c)* $POST\text{-}C3_2^2\bar{C}3_2^2$ *(*$\pi/2_x 2\pi_{-y} 3\pi/2_x$ *elements), 30 kHz rf field strength,* $10kHz$ *spinning (open circles) and* $C3_1^1\bar{C}3_1^1$ *(*$2\pi_x$ *elements), 30 kHz rf field strength, 10 kHz spinning (crosses), (b,d)* $C3_2^2\bar{C}3_2^2$ *(*$2\pi_x$ *elements),* $45.45kHz$ *rf field strength,* $30.3kHz$ *spinning (crosses) and* $EXPORT\text{-}C6_4^2$ *(*$C=3\omega_r/2, B=-\omega_r/2$ *)at* $30.3kHz$ *spinning (open circles).*

Chapter 4

Heteronuclear Decoupling

We can only see a short distance ahead, but we can see plenty there that needs to be done.
– Alan Turing

As we discussed in the chapter-1, decoupling is one of the essential parts of an NMR experiment and there have been many attempts to design a good decoupling pulse sequence. Different approaches have been used to achieve promising results for various rotor frequencies. Like, there are a number of sequences inspired by the two pulse phase modulated decoupling sequence (TPPM). This was the first heteronuclear multiple-pulse decoupling sequence, generally applicable in solids with a dense homonuclear coupling network. TPPM is easy to implement and optimize, it consists of two pulses with duration π and phase $+\phi$ and $-\phi$. Hence experimental optimization of the sequence requires a two-parameter optimization, namely the pulse length (π) and the phase ϕ of the pulses. It is not straightforward to predict the optimum decoupling parameters as a function of the MAS frequency and the rf-field amplitude. In practice, experimental optimization in the two-dimensional parameter space is required. Invention of TPPM was a mile stone in development of decoupling pulses with varying phases and amplitudes. As mentioned in the chapter-1 there are many variants of this sequence that were developed in the process of trying to understand and improve the basic sequence. FMPM, SPARC, SPINAL, SW_f-TPPM etc fall in this category. Another approach could be direct spectral optimization of the two parameters of a decoupling sequence on the spectrometer, techniques like continuous mode (CM) sequences are developed this way.
There have been other approaches besides the TPPM scheme to improve the decoupling in rotating solids. The symmetry-based rotor-synchronized CN_n^ν sequences can also be used for heteronuclear decoupling. $C12_2^{-1}$ has been experimentally implemented using hard pulses, this sequence requires a fixed ratio between the spinning frequency and the rf-field amplitude as discussed in the chapter-3. Use of adiabatic inversion pulses combined with a suitable phase cycle at slower MAS frequencies can also be an approach. Computer optimization of the spin dynamics for model spin systems led to the continuously phase-modulated DROOPY[14, 15] family of decoupling sequences. We are introducing the EXPORT-CN sequences and triple oscillatory field technique for elimination of the higher order static terms. The theory

and simulations followed by some experimental results are presented in this chapter.

4.1 EXPORT-CN as a decoupling sequence

In the previous chapter we saw how the combination of symmetry based pulses and multiple oscillating fields gives better results for homonuclear recoupling. Now our aim is to use those pulses for heteronuclear decoupling. We see from the selection rules that many of these sequences don't allow heteronuclear terms and CSA terms in first order only homonuclear coupling terms are allowed along with J-coupling and isotropic chemical shift. Now we will analyze the second order terms[20].
The selections rules for second order terms are

$$m_1 n - \mu_1 \nu - \mu_1 n \frac{B}{\omega_r} \neq Nz \tag{4.1}$$

AND

$$m_1 n - \mu_1 \nu - \mu_1 n \frac{B}{\omega_r} \neq Nz \tag{4.2}$$

AND

$$(m_1 + m_2) n - (\mu_1 + \mu_2) \nu - (\mu_1 + \mu_2) n \frac{B}{\omega_r} \neq Nz \tag{4.3}$$

where the N, n, ν and B are the pulse sequence parameters and m_1, m_2 and μ_1, μ_2 are space and spin indices for the two terms which are involved in the cross term. The derivation is given in appendix A. So the second order cross term of interactions Λ_1, Λ_2 is zero if above equations are satisfied. The expression for the scaling factor is

$$k = \frac{n}{2i\tau_c^2}[k^{B(12)}_{\substack{l_1,m_1,\lambda_1,\mu_1 \\ l_2,m_2,\lambda_2,\mu_2}} S^{\triangle}_{\substack{l_1,m_1,\lambda_1,\mu_1 \\ l_2,m_2,\lambda_2,\mu_2}} + k^{B(1)}_{l_1,m_1,\lambda_1,\mu_1} k^{B(2)}_{l_2,m_2,\lambda_2,\mu_2} S^{\square}_{\substack{l_1,m_1,\lambda_1,\mu_1 \\ l_2,m_2,\lambda_2,\mu_2}}] \tag{4.4}$$

with $k^{B(i)}_{l_i,m_i,\lambda_i,\mu_i}$ and $k^{B(ij)}_{\substack{l_i,m_i,\lambda_i,\mu_i \\ l_j,m_j,\lambda_j,\mu_j}}$ defined as

$$k^{B(i)}_{l_i,m_i,\lambda_i,\mu_i} = d^{l_i}_{m_i,0}(\beta_{RL}) \int_0^{\tau_c} dt e^{i(\mu_i\gamma_0 - Bt + m\omega_r t)} d^{\lambda_i}_{\mu_i,0}(-\omega_{rf} t)$$

$$k^{B(ij)}_{\substack{l_i,m_i,\lambda_i,\mu_i \\ l_j,m_j,\lambda_j,\mu_j}} = d^{l_i}_{m_i,0}(\beta_{RL}) d^{l_j}_{m_i,0}(\beta_{RL}) \int_0^{\tau_c} dt_1 \int_0^{t_1} dt_2 e^{i((\mu_i\gamma_0 + \mu_j\gamma_0') - B(t_1+t_2)) + (m_i t_1 + m_j t_2)\omega_r}$$
$$d^{\lambda_i}_{\mu_i,0}(-\omega_{rf} t_1) d^{\lambda_j}_{\mu_j,0}(-\omega_{rf} t_2)$$

The numerical values of some scaling factors were calculated using MATHEMATICA to get a good decoupling sequence. In the table 4.1 the scaling factors for 4 different sequences are listed and the sequence $C12^0_2 + EXP(B = -1/2)$ was giving the best results both on the simulations as well as on the spectrometer as discussed section 4.3.

4.2 Triple oscillating fields

The EXPORT$(B = -1/2) - C12^0_2$ sequence gives good decoupling as it has both abilities, the recoupling of homonuclear interactions and averaging higher order cross

Table 4.1: *Scaling factors of homonuclear coupling terms (l, m, λ, μ) and sum of scaling factors of all allowed second order $DD \times CSA$ terms*

term	$C12_2^{-1}$	$C12_2^0 + EXP(B = -1/2)$	$C12_2^1 + EXP(B = -1)$	$C12_2^{-3}$
2,-1,2,2	0.16999	0.17677	0.16999	0
2,1,2,-2	0.16999	0.17677	0.16999	0
second order	0.0123	0.0094	0.0092	0.0098

terms of $DD \times CSA$. To remove these higher order terms more efficiently we tried to extend this concept of additional oscillatory field and included a third perpendicular field. This sequence is called Triple Oscillatory Field (TOFU), earlier similar sequence was used to recouple isoCS and decouple CSA [18] but this time we changed the magnitude of the three fields. TOFU$(B = -1/2, A = 1/4)$ allows less number of terms in higher order but at the expense of less recoupling of homonuclear interaction. Nonetheless, the suppression of the higher orders terms is very good and the role of homonuclear recoupling is not yet clear, so we can afford the loss in recoupling. The sequence showed further improvement in performance than EXPORT$(B = -1/2) - C12_2^0$.
The Hamiltonian for TOFU$(B = -1/2, A = 1/4)$ is as follows:

$$H^{rf}(t) = CI_x + Be^{-iCI_xt}I_ye^{iCI_xt} + Ae^{-iCI_xt}e^{-iCI_yt}I_ze^{iCI_yt}e^{iCI_xt} \tag{4.5}$$

It is not very difficult to see by going by analogy of symmetry or EXPORT-CN sequences that the Hamiltonian of any given interaction will attend following form in this frame. Here we have to do three frame transformations starting from the Lab frame.

$$\tilde{\tilde{H}}^{\Lambda}_{lm\lambda\mu} = \omega^{\Lambda}_{lm}e^{i(m\omega_rt+\mu\gamma_0)}T^{\Lambda}_{\lambda\mu'}e^{i\frac{2\pi(mn-\mu'\nu)q}{N}}d^{\lambda}_{\mu,0}(-Ct)d^{\lambda}_{\mu',0}(-Bt) \tag{4.6}$$

Now there are two dummy indices μ and μ' so one has to sum over μ to get scaling factor of one allowed term which means μ' is fixed. This way the second order calculations become much more tedious as there we have two extra indices therefore we did the analysis of TOFU$(B = -1/2, A = 1/4)$ using product operators where one can see that many second order cross terms between CSA and DD which were being recoupled in case of EXPORT$(B = -1/2) - C12_2^0$ are now averaging out due to the third field A. We took $A = \omega_r/4$ and $B = -\omega_r/2$ as by taking this maximum no. terms get canceled. This way it require very less support from homonuclear coupling to average out the second order terms may be it is still important to remove even higher order terms like third order.
To justify the choice of the small oscillating fields A and B we will look on the $DD \times CSA$ and $DD \times DD$ terms in the frame of this pulse sequence. Starting with a Hamiltonian $H^D = DI_zS_z$ (here D is the dipolar coupling constant) if we apply all the three transformations to get into frame of (4.5), the final expression is as follows.

$$\begin{aligned}\tilde{\tilde{H}}^D = D[&I_z\cos(Ct)\cos(Bt) + I_x\{\cos(Ct)\sin(Bt)\sin(At) + \sin(Ct)\sin(At)\} \\ &+ I_y\{\cos(Ct)\sin(Bt)\sin(At) - \sin(Ct)\cos(At)\}]S_z\end{aligned} \tag{4.7}$$

In the above equation we did not included the spatial part which is not affected by these frame transformations. The spatial part also had a modulation in it with a frequency $m\omega_r$ ($m \in \{-2, -1, 1, 2\}$). Assuming C is large enough so that it cannot match with any linear combination of the rest of the frequencies than the first order Hamiltonian is zero as there is no static term.
The second order terms were calculated according to average Hamiltonian theory (2.5). The terms in second order are modulating with frequencies $(2B + A + m\omega_r), (B + A + m\omega_r)$ and $(A + m\omega_r)$ now if we fix value of $B = \frac{1}{2}\omega_r$ then there following cases for different values of A for :

- $A = 0$ and $m = -1$ which corresponds to case of EXPORT$(B = -1/2) - C12_2^0$, the terms modulating with $2B + A - \omega_r = 2B - \omega_r$ get recouple for $B = \frac{1}{2}\omega_r$.

- $A = B$ and $m = -1$ the terms modulating with $B + A - \omega_r = 2B - \omega_r$ get recouple for $B = \frac{1}{2}\omega_r$.

- $A = \frac{1}{4}\omega_r$ and $B = \frac{1}{2}\omega_r$ all the terms are modulating for all values of m.

For other values of A the simulations showed that the performance decreases this may be because of decreases in scaling factor. To confirm that analytically one has to do the complete integration with taking all the constants into consideration, here we only looked at different frequencies coming out after the double integration.

4.3 Role of homonuclear coupling in heteronuclear decoupling

The role played by homonuclear coupling in heteronuclear decoupling is still not very clear. In the literature one can find arguments for both the sides whether it is useful or it makes it more difficult. The analysis of $C12_2^{-1}$ sequence [16] shows that it exploits the homonuclear coupling to truncate the heteronuclear interaction. By looking at $C12_2^{-1}$ and $C12_2^{-3}$ sequences, it is evident that recoupling can make quite difference in decoupling performance as the former works marginally better due to its capability of using homonuclear couplings. The two sequences allow equal number of second order terms and both of them average out first order heteronuclear and CSA terms but the later one does not recouple first order homonuclear interaction whereas the first one does.Whereas some analysis [8] [14] show that presence of homonuclear coupling make the situation complicated to decouple the heteronuclear interactions.
Analytically, it can be seen that homonuclear coupling terms do not commute with the cross terms of heteronuclear coupling and CSA and this non-commuting behavior can be useful in the truncation of some higher order terms which could not be averaged out by the MAS and the decoupling pulse sequences. On the other hand homonuclear interactions can also lead to some static higher order cross terms with heteronuclear coupling causing a line broadening in the spectra.

To analyze the situation we used simulations. We considered sequences which suppress higher order cross terms along with recoupling capability for homonuclear dipolar couplings ($C12_2^{-1}$ and EXPORT($B = -1/2$)$-C12_2^0$) and sequence which removes the cross terms effectively but without significant recoupling of first order homonuclear interaction (TOFU(B=-1/2, A=1/4)). It was observed that if we include the homonuclear couplings in the simulations then it causes slight decrement in the decoupling efficiencies of all the sequences see Figure 4.1. Also if we observe closely, the loss due to the introduction of the homonuclear coupling is less in case of the TOFU($B = -1/2, A = 1/4$) than in the EXPORT and $C12_2^{-1}$. So one explanation is that EXPORT and $C12_2^{-1}$ recouples first order homonuclear terms which cause more damage in their decoupling profiles. In the case of TOFU($B = -1/2, A = 1/4$) there is not much reduction in peak height due to these homonuclear interactions as it averages them out. However, the spin systems in the simulations are not a very good model to simulate a real situation and it may happen that a larger network of homonuclear couplings truncates the cross terms with heteronuclear couplings. Therefore to deduce any conclusion from the simulations we have to use some larger spin systems where we can see whether the first order terms truncation effect can overtake the loss due to generation of static terms or not.

Experimentally, we see that EXPORT($B = -1/2$)$- C12_2^0$ which has a good recou-

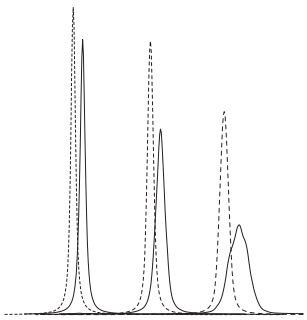

Figure 4.1: *Decoupling profiles of TOFU($B = -1/2, A = 1/4$), EXPORT($B = -1/2$)$- C12_2^0$ and $C12_2^{-1}$ with a spin system consisting of 3 protons and 1 carbon with and without presence of homonuclear couplings. The solid lines present the presence of homonuclear coupling and the dashed ones are for the cases when we excluded the homonuclear interactions from the simulations. The left most two peaks correspond to the TOFU($B = -1/2, A = 1/4$) sequence, middle ones to EXPORT($B = -1/2$)$- C12_2^0$ and the right most two peaks are for $C12_2^{-1}$ sequence. All the other parameters are same for all the cases as described in section 4.4*

pling profile for the homonuclear terms is doing well in decoupling. The comparison of EXPORT($B = -1/2$)$- C12_2^0$ with $C12_2^{-1}$ shows that the former is better in both recoupling of homonuclear interactions and decoupling of heteronuclear interactions. Also $C12_3^{-3}$ performs poorly for decoupling although it allows very less number of

second order terms and the sum of the scaling factors of these terms is also very less, the reason for this may be the less scaling factor for first order homonuclear terms see Table 4.1. This behavior of $C12_3^{-3}$ makes it more difficult to answer the question of role of homonuclear couplings in heteronuclear decoupling.

4.4 Simulations and Experimental Results

Here we show the performances of these sequences with the help of simulations and experimental graphs. In all the figures, we shifted the graphs for different pulse sequences for the sake of clarity in the comparison otherwise the resonances are at same frequencies for all the cases. The simulation on SIMPSON vindicate that the oscillating fields are very effective in removing higher order terms. A spin system consisting of 4 spins ($1^{13}C$ and 3^1H) was taken with a heteronuclear coupling between ^{13}C and ^1H equal to $23.3kHz$ and the three homonuclear couplings were $21.3kHz, 3880Hz$ and $6900Hz$. Crystal file rep144 and 5 gamma angles were included. All the simulations were at rotor frequency $11.111kHz$. The comparison of $C12_2^{-1}$, EXPORT$(B = -1/2) - C12_2^0$ and TOFU$(B = -1/2, A = 1/4)$ is shown in figure 4.2. The gain is very high in the simulation by adding a oscillating field however in the experiments the difference was not that much. This may be because of the complexity in the implementation of these new sequences as their amplitude and phases both are modulating.

To get the optimum value of the third field in case of TOFU$(B = -1/2, A = 1/4)$,

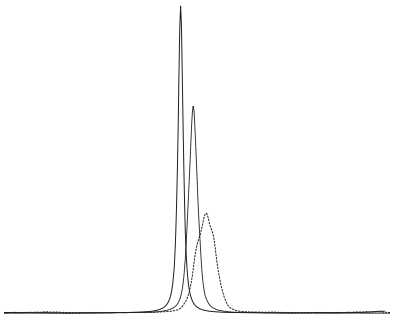

Figure 4.2: *Comparison of TOFU$(B = -1/2, A = 1/4)$ (the left most), EXPORT$(B = -1/2) - C12_2^0$ (in the middle)and $C12_2^{-1}$ (the right most) simulations on SIMPSON. All the cases are with same spinning so rf power is almost same for the three pulses. The peaks are at same resonance these are shifted for the sake of visibility.*

some simulations were done for various values of A and it was observed that it gives maximum decoupling at $A = 1/4$ (Figure 4.3) which is supported theoretically is section 4.2.

Decoupling experiments were performed to compare the performances of these new

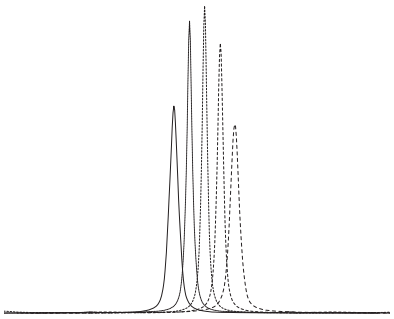

Figure 4.3: *Simulations for different values of A for TOFU sequence the value of B is fixed at* $-1/2$*. For* $A = 0, 1/8, 1/4, 3/8$ *and* $1/2$ *respectively from left to right it is observe that at* $1/4$ *the maxima is obtained.*

decoupling sequences among themselves and with TPPM. In the fig 4.4(a) we show the performances of $C12_2^{-1}$, EXPORT$(B = -1/2) - C12_2^0$, TOFU$(B = -1/2, A = 1/4)$ and TPPM. The experiments were performed on wide bore Bruker Avance 400MHz (9.4T) spectrometer with a double resonance solid-state probe on a $4mm$ rotor at a spinning frequency of $11.111kHz$. The sample was alanine (α, β labeled). The cross polarization was optimized at a power level of $25kHz$ on the protons with 80% ramp and on the carbon channel with the optimum power was $41.6kHz$. The decoupling power used was almost $66kHz$ for all the pulse sequences. The modulating fields were applied using the waves whereas the TPPM is using the standard hard pulses. Here we used TPPM15 so that the flip angle was 15 degrees. The results are shown in figure 4.4(a). Here the TPPM is showing the best performance follwed by TOFU$(B = -1/2, A = 1/4)$ then EXPORT$(B = -1/2) - C12_2^0$ and the symmetry based $C12_2^{-1}$. So the small modulating fields are improving the performance of the symmetry based sequences due to reduction in the second order scaling factors and by introducing the third field we are able to get results almost equal to the TPPM.

In figure 4.4(b) the comparison of the new pulses with TPPM is shown this time the rotor frequency is $11.7kHz$ consequently the rf power is also changed to $70.2kHz$ all the parameters are optimized for every case. Here we can see that the TOFU$(B = -1/2, A = 1/4)$ is doing slightly better than TPPM and the EXPORT$(B = -1/2) - C12_2^0$ is also comparable to it.

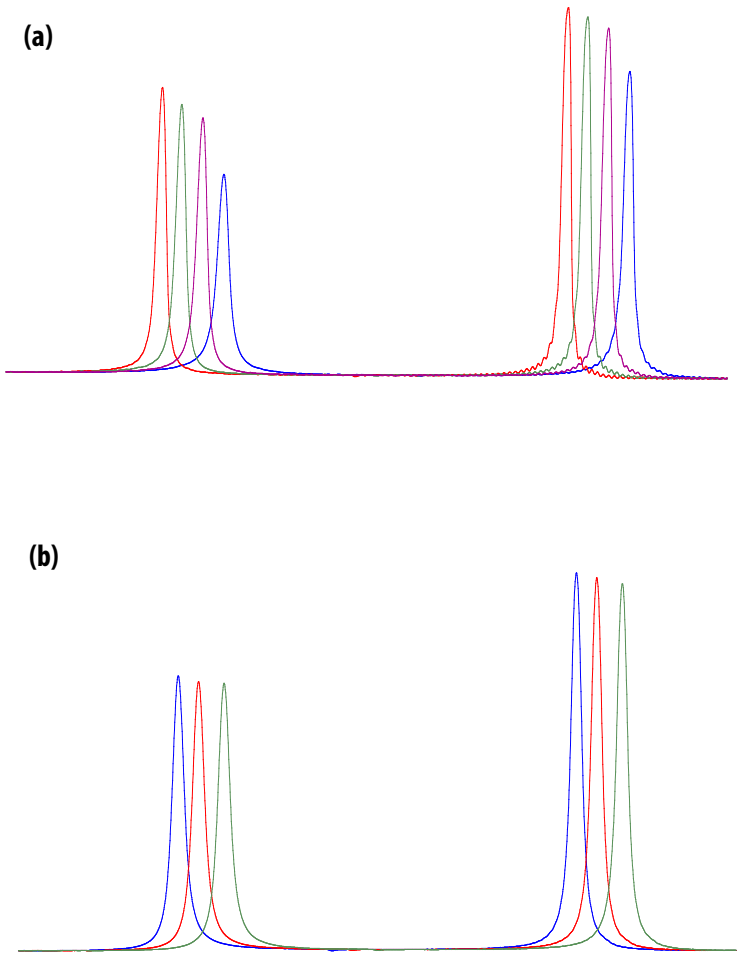

Figure 4.4: *(a)Comparison of symmetry based* $C12_2^{-1}$*,* $EXPORT(B = -1/2) - C12_2^0$*,* $TOFU(B = -1/2, A = 1/4)$ *and TPPM at* $11.111kHz$ *spinning frequency with a rf power of* $66.6kHz$ *on a* $400MHz$ *spectrometer. Alanine* $(\alpha, \beta$ *labeled) is used in* $4mm$ *rotor. Red line is for TPPM, green-*$TOFU(B = -1/2, A = 1/4)$*, purple-*$EXPORT(B = -1/2) - C12_2^0$ *and the blue one is for* $C12_2^{-1}$*.*
(b)Decoupling performances of $TOFU(B = -1/2, A = 1/4)$*, TPPM and* $EXPORT(B = -1/2) - C12_2^0$ *at* $11.7kHz$ *rotor frequency which means rf power is around* $70.2kHz$ *for all the three sequences. Experiments were performed on a* $400MHz$ *magnet* $4mm$ *solid-state rotor was used. The sample is alanine* $(\alpha, \beta$ *labeled). The left most blue line is for* $TOFU(B = -1/2, A = 1/4)$*, the red in the middle indicates the TPPM and the right most green line corresponds to the* $EXPORT(B = -1/2) - C12_2^0$ *sequence.*

Chapter 5

Conclusions

Some important observations and conclusions can be made on the basis of the results presented in this work. The recoupling capability of EXPORT-CN sequences at low rf power and high rotor frequency is indubitably good. We showed here that the addition of a modulating field to the symmetry based sequences lead to a significant improvement in its recoupling performance. If we have a symmetry based sequence which allows only desired terms (interactions) but not very effective due to low scaling factor then using EXPORT-CN one can keep the same selection rules and enhance the scaling factors with the help of the extra modulating field. It should be noted that this may not be always possible and also there is no assurance that the there will be significant gain in each and every case, so one has to choose the sequence carefully such that there is a scope of increment in scaling factor by addition of the modulating field.
Secondly, these new pulses can be use for decoupling with different parameters. For choosing a good decoupling pulse from the EXPORT-CN family one may look first on the allowed terms and then the second order scaling factors of $DD \times CSA$ terms. Here we showed that EXPORT$(B = -1/2) - C12_2^0$ is a sequence which averages all the first order heteronuclear and CSA terms and allows very less no. of second order terms. These two properties are same as $C12_2^{-1}$ but taking advantage of the extra modulations, we were able to lower the second order scaling factors further which results in better decoupling as shown by experimental results.
It is also evident that the averaging of second order terms using a third oscillating field reduces the line width effectively. The experimental performance of TOFU is almost same as the TPPM and even slight gain over it for certain spinning frequencies. However, TOFU does far better on simulations, possible reasons for this decay on the spectrometer may be the rf inhomogeneity and the way of implementation of these modulating rf fields.
The role played by the first order homonuclear coupling terms is important for the development of a decoupling pulse sequence. The EXPORT$(B = -1/2) - C12_2^0$ and $C12_2^{-1}$ have good homonuclear recoupling profiles which seems to help them in their heteronuclear decoupling efficiency. But the simulations do not favor this argument as for a spin systems with 3 or 4 spins the picture is apparently reverse. Also the decoupling performance of TOFU, which does not recouple homonuclear interaction,

is better than the EXPORT($B = -1/2$) $- C12_2^0$ and $C12_2^{-1}$. This indicates that the most effective way to decouple is by removing the higher order cross terms.

References

[1] A. L. Bloom, J. N. Shoolery, Effects of perturbing radiofrequency fields on nuclear spin coupling, Phys. Rev. 97 (5) (1955) 1261–.
URL http://link.aps.org/doi/10.1103/PhysRev.97.1261

[2] A. J. Shaka, J. Keeler, R. Freeman, Evaluation of a new broadband decoupling sequence: Waltz-16, Journal of Magnetic Resonance (1969) 53 (2) (1983) 313–340.
URL http://www.sciencedirect.com/science/article/B7GXD-4CRG7KN-PS/2/a9d6b51fc2141c6d678d119776e201fc

[3] A. J. Shaka, C. J. Lee, A. Pines, Iterative schemes for bilinear operators; application to spin decoupling, Journal of Magnetic Resonance (1969) 77 (2) (1988) 274–293.
URL http://www.sciencedirect.com/science/article/B7GXD-4CRGDYS-D3/2/887f9a96b013c0534d951049ba43537a

[4] A. J. Shaka, P. B. Barker, R. Freeman, Computer-optimized decoupling scheme for wideband applications and low-level operation, Journal of Magnetic Resonance (1969) 64 (3) (1985) 547–552.
URL http://www.sciencedirect.com/science/article/B7GXD-4CRGDM8-9D/2/efb75774576eaa8cb2b02e904fde3578

[5] E. Kupce, R. Freeman, Adiabatic pulses for wideband inversion and broadband decoupling, Journal of Magnetic Resonance, Series A 115 (2) (1995) 273–276.
URL http://www.sciencedirect.com/science/article/B6WJY-45S997T-5G/2/a15a876f98d5100f76f133e83243b583

[6] H. Arthanari, G. Wagner, N. Khaneja, Heteronuclear decoupling by multiple rotating frame technique, Journal of Magnetic Resonance 209 (1) (2011) 8–18.
URL http://www.sciencedirect.com/science/article/B6WJX-51MSRC2-1/2/98a931c65c30e1d56385cd704b531455

[7] E. R. ANDREW, A. BRADBURY, R. G. EADES, Nuclear magnetic resonance spectra from a crystal rotated at high speed, Nature 182 (4650) (1958) 1659–1659.
URL http://dx.doi.org/10.1038/1821659a0

[8] M. Ernst, Heteronuclear spin decoupling in solid-state nmr under magic-angle sample spinning, Journal of Magnetic Resonance 162 (1) (2003) 1–34.
URL http://www.sciencedirect.com/science/article/B6WJX-488NW6X-4/2/b7c251d53ff2926dd937a2e6ba50fc71

[9] A. E. Bennett, C. M. Rienstra, M. Auger, K. V. Lakshmi, R. G. Griffin, Heteronuclear decoupling in rotating solids, J. Chem. Phys. 103 (16) (1995) 6951–6958.
URL http://link.aip.org/link/?JCP/103/6951/1

[10] Z. Gan, R. Ernst, Frequency- and phase-modulated heteronuclear decoupling in rotating solids, Solid State Nuclear Magnetic Resonance 8 (3) (1997) 153–159.
URL http://www.sciencedirect.com/science/article/B6THK-3ST27YN-3/2/500e8f2feeac0f614c53d0c81d7e3797

[11] K. Takegoshi, J. Mizokami, T. Terao, 1h decoupling with third averaging in solid nmr, Chemical Physics Letters 341 (5-6) (2001) 540–544.
URL http://www.sciencedirect.com/science/article/B6TFN-43B8K6T-V/2/972d0d5ccc036821a5d8499836b0e672

[12] B. M. Fung, A. K. Khitrin, K. Ermolaev, An improved broadband decoupling sequence for liquid crystals and solids, Journal of Magnetic Resonance 142 (1) (2000) 97–101.
URL http://www.sciencedirect.com/science/article/B6WJX-45F4W9G-B1/2/3882f88d9d204c7e35eb845563c88778

[13] R. S. Thakur, N. D. Kurur, P. Madhu, Swept-frequency two-pulse phase modulation for heteronuclear dipolar decoupling in solid-state nmr, Chemical Physics Letters 426 (4-6) (2006) 459–463.
URL http://www.sciencedirect.com/science/article/B6TFN-4K4XJFR-4/2/95fa6fb444c425ee57df684c043d9037

[14] G. De Paëpe, P. Hodgkinson, L. Emsley, Improved heteronuclear decoupling schemes for solid-state magic angle spinning nmr by direct spectral optimization, Chemical Physics Letters 376 (3-4) (2003) 259–267.
URL http://www.sciencedirect.com/science/article/B6TFN-4903KMP-1/2/c122c1648ff0df750cdfff2c38983c4e

[15] G. De Paepe, A. Lesage, L. Emsley, The performance of phase modulated heteronuclear dipolar decoupling schemes in fast magic-angle-spinning nuclear magnetic resonance experiments, J. Chem. Phys. 119 (9) (2003) 4833–4841.
URL http://link.aip.org/link/?JCP/119/4833/1

[16] M. Eden, M. H. Levitt, Pulse sequence symmetries in the nuclear magnetic resonance of spinning solids: Application to heteronuclear decoupling, J. Chem. Phys. 111 (4) (1999) 1511–1519.
URL http://link.aip.org/link/?JCP/111/1511/1

[17] A. B. Nielsen, L. A. StraasÃÿ, A. J. Nieuwkoop, C. M. Rienstra, M. Bjerring, N. C. Nielsen, Broadband heteronuclear solid-state nmr experiments by exponentially modulated dipolar recoupling without decoupling, The Journal of Physical Chemistry Letters 1 (13) (2010) 1952–1956.
URL http://dx.doi.org/10.1021/jz100564j

[18] N. Khaneja, N. C. Nielsen, Triple oscillating field technique for accurate distance measurements by solid-state nmr, J. Chem. Phys. 128 (1) (2008) 015103–8.
URL http://link.aip.org/link/?JCP/128/015103/1

[19] G. De Paëpe, D. Sakellariou, P. Hodgkinson, S. Hediger, L. Emsley, Heteronuclear decoupling in nmr of liquid crystals using continuous phase modulation, Chemical Physics Letters 368 (5-6) (2003) 511–522.
URL http://www.sciencedirect.com/science/article/B6TFN-47GJ0R8-1/2/b2d95f699b9f6133393655e287728d90

[20] A. Brinkmann, M. Eden, Second order average hamiltonian theory of symmetry-based pulse schemes in the nuclear magnetic resonance of rotating solids: Application to triple-quantum dipolar recoupling, J. Chem. Phys. 120 (24) (2004) 11726–11745.
URL http://link.aip.org/link/?JCP/120/11726/1

[21] A. B. Nielsen, S. K. Jain, N. C. Nielsen, Low-power homonuclear dipolar recoupling using supercycled symmetry-based and exponentially-modulated pulse sequences, Chemical Physics Letters 503 (4-6) (2011) 310–315.
URL http://www.sciencedirect.com/science/article/B6TFN-51TYF5R-1/2/ac151bcd9d92be3d1a3a076abc2fda6e

[22] W. Magnus, On the exponential solution of differential equations for a linear operator, Comm. Pure Appl. Math. 7 (4) (1954) 649–673.
URL http://dx.doi.org/10.1002/cpa.3160070404

[23] W. A. B. Evans, On some applications of the magnus expansion in nuclear magnetic resonance, Annals of Physics 48 (1) (1968) 72–93.
URL http://www.sciencedirect.com/science/article/B6WB1-4DF549V-232/2/010fddb9a12b7f9c910ea12d8e78b1c2

[24] U. Haeberlen, J. S. Waugh, Coherent averaging effects in magnetic resonance, Phys. Rev. 175 (2) (1968) 453–.
URL http://link.aps.org/doi/10.1103/PhysRev.175.453

[25] M. Hohwy, N. C. Nielsen, Systematic design and evaluation of multiple-pulse experiments in nuclear magnetic resonance spectroscopy using a semi-continuous baker–campbell–hausdorff expansion, J. Chem. Phys. 109 (10) (1998) 3780–3791.
URL http://link.aip.org/link/?JCP/109/3780/1

[26] E. Wigner, On unitary representations of the inhomogeneous lorentz group, The Annals of Mathematics 40 (1) (1939) pp. 149–204.
URL http://www.jstor.org/stable/1968551

[27] L. A. Straaso, M. Bjerring, N. Khaneja, N. C. Nielsen, Multiple-oscillating-field techniques for accurate distance measurements by solid-state nmr, J. Chem.

Phys. 130 (22) (2009) 225103–14.
URL http://link.aip.org/link/?JCP/130/225103/1

Appendix A

Second order selection rules and scaling factors

We have the Hamiltonian in EXPORT-CN frame (3.18)using the AHT it can be easily seen that the second order Hamiltonian for $(q+1)^{th}$ cycle for two given interactions (Λ_1, Λ_2) is given by

$$\bar{\bar{\tilde{H}}}^{\Lambda_1\Lambda_2(2)}_{\substack{l_1m_1\lambda_1\mu_1\\ l_2m_2\lambda_2\mu_2}} = \frac{1}{2i\tau_c}\Gamma^{B(12)}_{\substack{l_1,m_1,\lambda_1,\mu_1\\ l_2,m_2,\lambda_2,\mu_2}} e^{i\frac{2\pi M^{12}_B q}{N}}[T^{\Lambda_1}_{\lambda_1\mu_1}, T^{\Lambda_2}_{\lambda_2\mu_2}] \tag{A.1}$$

where Ms and Γs are defined as

$$M^i_B = m_i n - \mu_i\nu - \mu_i n\frac{B}{\omega_r} \tag{A.2}$$

$$M^{ij}_B = (m_i+m_j)n - (\mu_i+\mu_j)\nu - (\mu_i+\mu_j)n\frac{B}{\omega_r} \tag{A.3}$$

$$\Gamma^{B(i)}_{l_i,m_i,\lambda_i,\mu_i} = \int_0^{\tau_c} dt\omega^{\Lambda_i}_{l_im_i}(t)e^{i(\mu_i\gamma_0 - Bt)}d^{\lambda}_{\mu_i,0}(\omega_r f t) \tag{A.4}$$

$$\Gamma^{B(ij)}_{\substack{l_i,m_i,\lambda_i,\mu_i\\ l_j,m_j,\lambda_j,\mu_j}} = \int_0^{\tau_c} dt_1\int_0^{t_1} dt_2\omega^{\Lambda_i}_{l_im_i}\omega^{\Lambda_j}_{l_jm_j}e^{i((\mu_i+\mu_j)\gamma_0 - B(t_1+t_2))}d^{\lambda_i}_{\mu_i,0}(\omega_r f t_1)d^{\lambda_j}_{\mu_j,0}(\omega_r f t_2) \tag{A.5}$$

To get the total second order Hamiltonian, the summations over Λ_1 and Λ_2 should be carried out. Again in the similar fashion as we did for first order the semi continuous BCH theory can be utilized to get the second order Hamiltonian for the entire sequence time. This time there are two parts (2.11).

$$\text{part-1 } \bar{\bar{\tilde{H}}}^{\Lambda_1\Lambda_2(2)}_{\substack{l_1m_1\lambda_1\mu_1\\ l_2m_2\lambda_2\mu_2}} = \sum_{q=0}^{N-1}\frac{1}{\tau_c}\Gamma^{B(12)}_{\substack{l_1,m_1,\lambda_1,\mu_1\\ l_2,m_2,\lambda_2,\mu_2}} e^{i\frac{2\pi M^{12}_B q}{N}}[T^{\Lambda_1}_{\lambda_1\mu_1}, T^{\Lambda_2}_{\lambda_2\mu_2}] \tag{A.6}$$

$$\text{part-2 } \bar{\bar{\tilde{H}}}^{\Lambda_1\Lambda_2(2)}_{\substack{l_1m_1\lambda_1\mu_1\\ l_2m_2\lambda_2\mu_2}} = \sum_{q=0}^{N-1}\frac{1}{2i\tau_c}\Gamma^{B(1)}_{l_1,m_1,\lambda_1,\mu_1}\Gamma^{B(2)}_{l_2,m_2,\lambda_2,\mu_2} e^{i\frac{2\pi M^1_B q}{N}}e^{i\frac{2\pi M^2_B q}{N}}[T^{\Lambda_1}_{\lambda_1\mu_1}, T^{\Lambda_2}_{\lambda_2\mu_2}] \tag{A.7}$$

Now to simplify it further and get the expressions of the second order scaling factor and the selection rules we will use following equalities. one can verify that

$$\sum_{i=1}^{N-1}\sum_{j=1}^{i-1} a^i b^j = \begin{cases} \frac{1}{1-a} & \text{if } a \neq 1, b = 1 \\ \frac{1}{1-b} & \text{if } b \neq 1, a = 1 \\ \frac{1}{2}N(N-1) & \text{if } a = 1, b = 1 \\ \frac{N(a-1)+1-a^N}{(1-a)(1-b)} & \text{if } a = \frac{1}{b} \neq 1 \\ \frac{(a-a^N)(1-ab)-(1-ab)(ab-(ab)^N)}{(1-a)(1-b)(1-ab)} & \text{if } a \neq 1, b \neq 1, ab \neq 1 \end{cases}$$

In case of $a^N = 1$ and $b^N = 1$ this gets simplified to

$$\sum_{i=1}^{N-1}\sum_{j=1}^{i-1} a^i b^j = \begin{cases} \frac{1}{1-a} & \text{if } a \neq 1, b = 1 \\ \frac{1}{1-b} & \text{if } b \neq 1, a = 1 \\ \frac{1}{2}N(N-1) & \text{if } a = 1, b = 1 \\ \frac{N}{(b-1)} & \text{if } a = \frac{1}{b} \neq 1 \\ 0 & \text{if } a \neq 1, b \neq 1, ab \neq 1 \end{cases}$$

If we define

$$S^{\triangle}_{\substack{l_1,m_1,\lambda_1,\mu_1 \\ l_2,m_2,\lambda_2,\mu_2}} = \frac{1}{N^2}\sum_{q=0}^{N-1} e^{i\frac{2\pi M_B^{12} q}{N}}$$

and

$$S^{\square}_{\substack{l_1,m_1,\lambda_1,\mu_1 \\ l_2,m_2,\lambda_2,\mu_2}} = \frac{1}{N^2}\sum_{q=0}^{N-1}\sum_{p=0}^{q-1} e^{i\frac{2\pi M_B^{1} q}{N}} e^{i\frac{2\pi M_B^{2} p}{N}}$$

then using the above mentioned equalities one can see that

$$S^{\triangle}_{\substack{l_1,m_1,\lambda_1,\mu_1 \\ l_2,m_2,\lambda_2,\mu_2}} = \begin{cases} \frac{1}{N} & \text{if } M_B^{12} = Nz \\ 0 & \text{if } M_B^{12} \neq Nz \end{cases}$$

and

$$S^{\square}_{\substack{l_1,m_1,\lambda_1,\mu_1\\ l_2,m_2,\lambda_2,\mu_2}} = \begin{cases} 0 & \text{if } \left(\begin{array}{c} M_B^{12} \neq Nz \\ \text{AND} \\ M_B^{1} \neq Nz \\ \text{AND} \\ M_B^{2} \neq Nz \end{array}\right). \\ -i\frac{\exp(-i\pi M_B^1/N)}{2N\sin(i\pi M_B^1/N)} & \text{if } \left(\begin{array}{c} M_B^{12} = Nz \\ \text{AND} \\ M_B^{1} \neq Nz \\ \text{AND} \\ M_B^{2} \neq Nz \end{array}\right). \\ -i\frac{\exp(-i\pi M_B^2/N)}{2N\sin(i\pi M_B^2/N)} & \text{if } \left(\begin{array}{c} M_B^{12} \neq Nz \\ \text{AND} \\ M_B^{1} = Nz \\ \text{AND} \\ M_B^{2} \neq Nz \end{array}\right). \\ -i\frac{\exp(-i\pi M_B^1/N)}{2N\sin(i\pi M_B^1/N)} & \text{if } \left(\begin{array}{c} M_B^{12} \neq Nz \\ \text{AND} \\ M_B^{1} \neq Nz \\ \text{AND} \\ M_B^{2} = Nz \end{array}\right). \\ \frac{N-1}{2N} & \text{if } \left(\begin{array}{c} M_B^{12} = Nz \\ \text{AND} \\ M_B^{1} = Nz \\ \text{AND} \\ M_B^{2} = Nz \end{array}\right). \end{cases}$$

The selection rules and the expressions for the calculations of the scaling factors can be obtained by rewriting the Hamiltonian as

$$\tilde{\tilde{H}}^{\Lambda_1\Lambda_2(2)}_{\substack{l_1m_1\lambda_1\mu_1\\ l_2m_2\lambda_2\mu_2}} = (\frac{1}{\tau_c} k^{B(12)}_{\substack{l_1,m_1,\lambda_1,\mu_1\\ l_2,m_2,\lambda_2,\mu_2}} S^{\triangle}_{\substack{l_1,m_1,\lambda_1,\mu_1\\ l_2,m_2,\lambda_2,\mu_2}} + \frac{1}{2i\tau_c} k^{B(1)}_{l_1,m_1,\lambda_1,\mu_1} k^{B(2)}_{l_2,m_2,\lambda_2,\mu_2} S^{\square}_{\substack{l_1,m_1,\lambda_1,\mu_1\\ l_2,m_2,\lambda_2,\mu_2}})$$
$$[[A^{\Lambda_1}_{l_1m_1}]^R T^{\Lambda_1}_{\lambda_1\mu_1}, [A^{\Lambda_2}_{l_2m_2}]^R T^{\Lambda_2}_{\lambda_2\mu_2}]$$

where the $k^{B(i)}_{l_i,m_i,\lambda_i,\mu_i}$ and $k^{B(ij)}_{\substack{l_i,m_i,\lambda_i,\mu_i\\ l_j,m_j,\lambda_j,\mu_j}}$ are defined as

$$k^{B(i)}_{l_i,m_i,\lambda_i,\mu_i} = d^{l_i}_{m_i,0}(\beta_{RL}) \int_0^{\tau_c} dt e^{i(\mu_i\gamma_0 - Bt + m\omega_r t)} d^{\lambda_i}_{\mu_i,0}(-\omega_{rf}t)$$

$$k^{B(ij)}_{\substack{l_i,m_i,\lambda_i,\mu_i\\ l_j,m_j,\lambda_j,\mu_j}} = d^{l_i}_{m_i,0}(\beta_{RL}) d^{l_j}_{m_i,0}(\beta_{RL}) \int_0^{\tau_c} dt_1 \int_0^{t_1} dt_2 e^{i((\mu_i\gamma_0+\mu_j\gamma_0') - B(t_1+t_2)) + (m_it_1+m_jt_2)\omega_r}$$
$$d^{\lambda_i}_{\mu_i,0}(-\omega_{rf}t_1) d^{\lambda_j}_{\mu_j,0}(-\omega_{rf}t_2)$$

It can be observed that the second order Hamiltonian is zero if

$$m_1 n - \mu_1 \nu - \mu_1 n \frac{B}{\omega_r} \neq Nz \tag{A.8}$$

AND

$$m_1 n - \mu_1 \nu - \mu_1 n \frac{B}{\omega_r} \neq Nz \tag{A.9}$$

AND

$$(m_1 + m_2) n - (\mu_1 + \mu_2) \nu - (\mu_1 + \mu_2) n \frac{B}{\omega_r} \neq Nz \tag{A.10}$$

As both $S^{\triangle}_{\substack{l_1,m_1,\lambda_1,\mu_1 \\ l_2,m_2,\lambda_2,\mu_2}}$ and $S^{\square}_{\substack{l_1,m_1,\lambda_1,\mu_1 \\ l_2,m_2,\lambda_2,\mu_2}}$ are zero in that case. For the scaling factors, this time we have two terms depending the values of Ss. Unlike the first order case Ss are not taking values only 1 or 0. To take the values Ss into consideration one has to take care of all the different cases. The scaling factors then can be calculated using the following equation.

$$k = \frac{n}{2i\tau_c^2} [k^{B(12)}_{\substack{l_1,m_1,\lambda_1,\mu_1 \\ l_2,m_2,\lambda_2,\mu_2}} S^{\triangle}_{\substack{l_1,m_1,\lambda_1,\mu_1 \\ l_2,m_2,\lambda_2,\mu_2}} + k^{B(1)}_{l_1,m_1,\lambda_1,\mu_1} k^{B(2)}_{l_2,m_2,\lambda_2,\mu_2} S^{\square}_{\substack{l_1,m_1,\lambda_1,\mu_1 \\ l_2,m_2,\lambda_2,\mu_2}}] \tag{A.11}$$

Appendix B

Low-power homonuclear dipolar recoupling using super-cycled symmetry-based and exponentially-modulated pulse sequences

Chemical Physics Letters 503 (2011) 310–315

Contents lists available at ScienceDirect

Chemical Physics Letters

journal homepage: www.elsevier.com/locate/cplett

Low-power homonuclear dipolar recoupling using supercycled symmetry-based and exponentially-modulated pulse sequences

Anders Bodholt Nielsen, Sheetal Kumar Jain, Niels Chr. Nielsen *

Center for Insoluble Protein Structures (inSPIN), Interdisciplinary Nanoscience Center (iNANO) and Department of Chemistry, Aarhus University, DK-8000 Aarhus C, Denmark

ARTICLE INFO

Article history:
Received 14 November 2010
In final form 27 December 2010
Available online 30 December 2010

ABSTRACT

Aimed at performing dipolar recoupling as part of biological solid-state NMR experiments without using excessively strong rf irradiation, we present a series of low-power supercycled symmetry-based and exponentially modulated pulse sequences facilitating efficient recoupling over specified chemical shift ranges even at high-speed spinning conditions. The experiments are designed through simple phase modulation of known 'lower-quality' symmetry-based pulse sequences or highly rf-demanding exponentially modulated recoupling experiments. The methods are described analytically and numerically and demonstrated experimentally by one- and two-dimensional correlation spectra of 2,3-$^{13}C_2$-*L*-alanine and the fibrillating-core decapeptide SNNFGAILSS of human Islet Amyloid Poly-Peptide (hIAPP, or amylin) uniformly ^{13}C,^{15}N-labeled at the FGAIL residues.

1. Introduction

Facilitated by increasingly strong magnetic fields, fast magic-angle spinning (MAS) equipment, and development of increasingly efficient pulse sequences for dipolar recoupling, solid-state NMR spectroscopy is gradually emerging as a very powerful method for determining structure and dynamics of biological macromolecules in the solid phase. Uniquely, the method allows for the establishment of atomic-resolution structural information for proteins residing in non-crystalline or liquous environments, such as membrane proteins [1,2] and amyloid fibrils [3,4]. Depending on the available amount of sample, the content of salt, and instrumental capabilities/preferences such studies have been carried out using widely different experimental conditions. This sets high demands to the flexibility and operational conditions for the fundamental dipolar recoupling techniques serving as key elements to transfer magnetization among spin species for assignment purposes and to probe molecular structure in terms of internuclear distances and dihedral angles.

Lately, considerable interest has been devoted to fast sample spinning experiments, in which case it is of fundamental importance to use recoupling methods operating without the need of intense ^1H decoupling [5–8] (however, typically at the expense of very strong rf fields on the involved low-γ nuclei such as ^{13}C and/or ^{15}N) and/or recoupling/diffusion methods requiring sufficiently low rf power on the $^{13}C/^{15}N$ channels to allow for simultaneous ^1H rf irradiation to ensure efficient decoupling [9–12]. Both strategies set high demands to the pulse engineering methods, for example, lately involving the introduction of advanced average Hamiltonian based multiple-oscillating field techniques [7,13–16] or pulse sequences designed using optimal control procedures [17–21].

In this Letter, we address the development of γ-encoded [22] low-power dipolar recoupling methods based on known design principles such as symmetry-based CN_ν^n recoupling [23–26] and multiple-oscillating field techniques [7,14,16]. Both are known to be demanding with respect to rf power when used in their original form, but when imbedded into simple supercycling scaffolds or systematically intertwined the demands to the rf power may be reduced significantly opening up for high-speed spinning applications as demonstrated in this Letter. We describe the basic principles of designing such experiments analytically and demonstrate the performance of a selected set of experiments numerically and experimentally using typical conditions for ^{13}C,^{15}N-labeled proteins.

2. Theory

A highly developed approach for design of efficient dipolar recoupling experiments to mediate transfer between ^{13}C spins is the symmetry-based CN_n^ν pulse sequences [23–26] which is formed by concatenation of N rf pulse elements distributed over n rotor periods ($\tau_r = 2\pi/\omega_r$ with ω_r being the angular spinning frequency) and the phase incremented systematically as $\phi_p = 2\pi np/N$ with $p = 0, 1, \ldots, N-1$. Using standard [23] $2\pi_x 2\pi_{-x}$ or a permutation–offset-stabilized (POST) [24] $\pi/2_x 2\pi_{-x} 3\pi/2_x$ basic elements, the rf field strength is $N\omega_r/2\pi$.

* Corresponding author.
E-mail addresses: ncn@inano.dk, ncn@chem.au.dk (N.C. Nielsen).

0009-2614/$ - see front matter © 2010 Elsevier B.V. All rights reserved.
doi:10.1016/j.cplett.2010.12.084

Within the Zeeman interaction frame, the internal nuclear spin Hamiltonian may be written as [25,26]

$$H(t) = \sum_{\Lambda,l,m,\lambda} H^{\Lambda}_{lm\lambda 0}(t); \qquad H^{\Lambda}_{lm\lambda 0}(t) = \omega^{\Lambda}_{lm}(t) T^{\Lambda}_{\lambda 0}, \tag{1}$$

where Λ represents a given nuclear spin interaction ($\Lambda = D$ dipole–dipole coupling $\Lambda = J$ scalar coupling, $\Lambda = \delta$ chemical shift), l and λ are rank of irreducible spherical tensors for the spatial and spin components, respectively, with indices m and μ (above the latter index is set to zero, while it later adopts other values; *vide infra*) taking values $m = -l, -l+1, ..., l$ and $\mu = -\lambda, -\lambda+1, ..., \lambda$. The angular frequency amplitude is given by $\omega^{\Lambda}_{lm}(t) = \omega^{\Lambda}_{lm} e^{im\omega_r t}$, introducing the Fourier components $\omega^{\Lambda}_{lm} = [R^{\Lambda}_{lm}]^R d^{(l)}_{m0}(\beta_{RL}) e^{-im\alpha_0}$, where $[R^{\Lambda}_{lm}]^R$ is the m'th component of the spatial tensor in the rotor-fixed frame R, β_{RL} the angle between the rotor axis and the static magnetic field in the laboratory frame L, α_0 the position of the rotor at time $t = 0$, and $d^{(l)}_{m0}(\beta_{RL})$ a l'th rank reduced Wigner element. In the interaction frame of the rf irradiation, the Hamiltonian transforms to

$$\tilde{H}^{\Lambda}_{lm\lambda\mu}(t) = \sum_{lm\lambda\mu} \tilde{H}^{\Lambda}_{lm\lambda\mu}(t - t^0_p) e^{i2\pi\frac{p}{N}(nm - v\mu)}, \tag{2}$$

with

$$\tilde{H}^{\Lambda}_{lm\lambda\mu}(t - t^0_p) = \omega^{\Lambda}_{lm} d^{\lambda}_{\mu 0}(-\beta_0(t - t^0_p)) e^{i\{m\alpha_r(t - t^0_p) + \mu\gamma_0\}} T^{\Lambda}_{\lambda\mu} \tag{3}$$

where the time t is within the p'th pulse sequence element ($t^0_p \leqslant t \leqslant^0_{p+1}$) of the CN^v_n pulse sequence with γ_0 and $\beta_0(t - t^0_p)$ referring to Euler angles describing the rf evolution angle $\omega_{rf}t$ and phase ϕ for the first element relating to the pulse sequence symmetry as outlined, e.g., in Ref. [26].

Through selection of the integers N, n, and v the CN^v_n symmetry-based pulse sequences offer great flexibility to selectively recouple desired parts of the internal nuclear spin Hamiltonian. The selection rule [23,25,26] is typically cast in terms of the first-order effective Hamiltonian

$$\overline{\tilde{H}}^{\Lambda(1)}_{lm\lambda\mu} = \frac{1}{\tau_c}\int_0^{\tau_c} \tilde{H}^{\Lambda}_{lm\lambda\mu}(t)dt = 0 \text{ if } mn - \mu v \neq NZ, \tag{4}$$

where Z is any integer and $\tau_c = n\tau_r = n2\pi/\omega_r$. In this notation, the various interactions are characterized by (l,λ) numbers: Homonuclear dipole–dipole coupling (2,2), homonuclear J coupling (0,0), isotropic chemical shift (0,1), chemical shift anisotropy and heteronuclear dipole–dipole coupling (2,1). A large number of symmetry-based pulse sequences have been designed using the selection rule in Eq. (4), starting with the $C7^1_2$ and POST-$C7^1_2$ pulse sequences [23,24] and later followed by a whole array of methods [25–27] with the effective Hamiltonian tailored by turning on and off certain interactions.

Among the many possible CN^v_n sequences, most focus has been devoted to those recoupling pure dipolar coupling or pure chemical shift Hamiltonians and sequences which may be used for decoupling. Such sequences typically require relatively large values of N to discriminate dipolar coupling and chemical shielding terms, with associated high demands to the rf power. An example is the original $C7^1_2$ pulse sequence, which recouples exclusively the dipolar $\overline{H}^{(1)}_{2,1,2,2}$ and $\overline{H}^{(1)}_{2,-1,2,-2}$ Hamiltonians to first order, while using an rf field strength of $7\omega_r$. We note that the rf field strength demands of such highly interaction-type selective symmetry-based recoupling sequences has been lowered somewhat using supercycling strategies [26] as well as design of novel pulse sequence elements by non-linear optimization [28] or optimal control procedures [20]. Our entry-point is to focus on the simpler $C3^1_1$ and $C3^1_2$ symmetries, for which it is possible to reduce the rf field strength radically at the expense of a much reduced selectivity with respect to recoupled terms which subsequently can be cleaned up through supercycling or combination with exponentially-modulated pulse elements.

For the first symmetry ($C3^1_1$), we observe reintroduction of the following homonuclear dipole–dipole coupling terms $\overline{H}^{(1)}_{2,-2,2,1}$, $\overline{H}^{(1)}_{2,-1,2,2}, \overline{H}^{(1)}_{2,1,2,-2}, \overline{H}^{(1)}_{2,2,2,-1}, \overline{H}^{(1)}_{2,-2,2,-2}, \overline{H}^{(1)}_{2,2,2,2}, \overline{H}^{(1)}_{2,-1,2,-1}$, and $\overline{H}^{(1)}_{2,1,2,1}$ in addition to the chemical shielding anisotropy or heteronuclear dipole–dipole coupling terms $\overline{H}^{(1)}_{2,-2,1,1}, \overline{H}^{(1)}_{2,-1,1,-1}, \overline{H}^{(1)}_{2,1,1,1}$, and $\overline{H}^{(1)}_{2,2,1,-1}$, as well as the isotropic chemical shift $\overline{H}^{(1)}_{0,0,1,0}$ and homonuclear J coupling $\overline{H}^{(1)}_{0,0,0,0}$ terms. Invoking now symmetry-based supercycling or so-called z-rotational decoupling [29] in form of $C3^1_1 e^{-i\pi I_z} C3^1_1 e^{i\pi I_z}$ (henceforth denoted $C3^1_1\overline{C3}^1_1$), all the elements recoupling $\mu = \pm 1$ will be eliminated. Accordingly, all chemical shielding anisotropy and heteronuclear dipole–dipole coupling terms as well as several of the homonuclear dipole–dipole coupling contributions will be removed. This leaves us with the operators $\overline{H}^{(1)}_{2,-2,2,-2}, \overline{H}^{(1)}_{2,-1,2,2}, \overline{H}^{(1)}_{2,1,2,-2}, \overline{H}^{(1)}_{2,2,2,2}, \overline{H}^{(1)}_{0,0,0,0}$, and $\overline{H}^{(1)}_{0,0,1,0}$ according to the selection in Eq. (4). Among these, the first-order chemical shielding term $\overline{H}^{(1)}_{0,0,1,0}$ will be averaged out through the $d^{\lambda}_{\mu 0}(-\omega_{rf}(t - t^0_p))$ term (Eq. (3)) by selecting a pulse sequence element with overall flip-angle being an integral number of 2π. The J-coupling term $\overline{H}^{(1)}_{0,0,0,0}$ will typical not disturb the spin evolution provided the aim is one-bond transfers among ^{13}C spins and the scaling factor of the dipole–dipole coupling is reasonably big. The recoupled dipolar Hamiltonian to first order takes the form

$$\overline{\tilde{H}}^{D(1)} = \overline{\tilde{\omega}}^{D}_{2,-2,2,-2} T^{D}_{2,-2} + \overline{\tilde{\omega}}^{D}_{2,2,2,2} T^{D}_{2,2} + \overline{\tilde{\omega}}^{D}_{2,1,2,-2} T^{D}_{2,-2} + \overline{\tilde{\omega}}^{D}_{2,-1,2,2} T^{D}_{2,2}, \tag{5}$$

with the coefficients $\overline{\tilde{\omega}}^{D}_{2,m,2,\pm 2} = \kappa^{(1)}_{2,m,2,\pm 2} [R^{\Lambda}_{lm}]^R e^{-im\alpha_0}$ and the scaling factors given by $|\kappa^{(1)}_{2,-2,2,-2}| = |\kappa^{(1)}_{2,2,2,2}| = 0.0581$ and $|\kappa^{(1)}_{2,1,2,-2}| = |\kappa^{(1)}_{2,-1,2,2}| = 0.1504$. The dominating latter coefficient largely ensures typical first-order Fourier component ($m = \pm 1$) encoded double-quantum dipolar recoupling as known from the vast majority of previous recoupling methods, here, however, with the rf field reduced to $3\omega_r$.

We note that z-rotations in the form of phase alternation or more extensive rotations around the z-axis may also eliminate a good fraction of the second-order Hamiltonians, e.g., entering as cross-terms between dipolar coupling and chemical shielding terms. A second-order term generally takes the form

$$\overline{\tilde{H}}^{\Lambda\Lambda'(2)}_{lm\lambda\mu,l'm'\lambda'\mu'} = \frac{1}{2i\tau_c}\int_0^{\tau_c} dt' \int_0^{t'} dt [\tilde{H}^{\Lambda}_{lm\lambda\mu}(t), \tilde{H}^{\Lambda'}_{l'm'\lambda'\mu'}(t')], \tag{6}$$

which in the case of cross-terms between chemical shift and dipolar coupling introduces second-rank spin operators according to the commutation relation $[T^{\delta}_{1,\mu}, T^{D}_{2,\mu'}] = \chi(\mu,\mu') T^{\delta\times D}_{2,\mu+\mu'}$ with $\chi(\mu,\mu') = -\chi(\mu',\mu)$ being μ' for $\mu = 0$ and $\mp\sqrt{\frac{6-\mu'(\mu'\pm 1)}{2}}$ for $\mu = \pm 1$ [30]. Of these terms, the terms with $\mu + \mu' = \pm 1$ will be eliminated by concatenating phase alternated elements as, e.g., in the $C3^1_1\overline{C3}^1_1$ pulse sequence.

The second symmetry ($C3^1_2$) recouples the homonuclear dipole–dipole coupling $\overline{H}^{(1)}_{2,-2,2,2}, \overline{H}^{(1)}_{2,-2,2,-1}, \overline{H}^{(1)}_{2,2,2,1}, \overline{H}^{(1)}_{2,2,2,-2}, \overline{H}^{(1)}_{2,-1,2,1}$, $\overline{H}^{(1)}_{2,-1,2,-2}, \overline{H}^{(1)}_{2,1,2,2}, \overline{H}^{(1)}_{2,1,2,-1}$, chemical shielding anisotropy and heteronuclear dipole–dipole coupling $\overline{H}^{(1)}_{2,-2,1,-1}, \overline{H}^{(1)}_{2,-1,1,1}, \overline{H}^{(1)}_{2,1,1,-1}, \overline{H}^{(1)}_{2,2,1,1}$, homonuclear J coupling $\overline{H}^{(1)}_{0,0,0,0}$, and isotropic chemical shielding $\overline{H}^{(1)}_{0,0,1,0}$ first-order terms. Similar to the case above the scaling factor for the isotropic chemical shift becomes $\kappa^{(1)}_{0,0,1,0} = 0$. Also here concatenation with a phase-reversed sequence, i.e. $C3^1_2 e^{-i\pi I_z} C3^1_2 e^{i\pi I_z}$ (denoted $C3^1_2\overline{C3}^1_2$), mediates elimination of all first- and second-order $\mu = \pm 1$ terms, leaving to first order the homonuclear dipole–dipole coupling $\overline{H}^{(1)}_{2,-2,2,2}, \overline{H}^{(1)}_{2,-1,2,-2}, \overline{H}^{(1)}_{2,1,2,2}, \overline{H}^{(1)}_{2,2,2,-2}$, and J

coupling $\overline{H}^{(1)}_{0,0,0,0}$ terms. The residual first-order dipolar Hamiltonian takes the form

$$\overline{\tilde{H}}^{D(1)} = \overline{\omega}^{D}_{2,2,2,-2}T^{D}_{2,-2} + \overline{\omega}^{D}_{2,-2,2,2}T^{D}_{2,2} + \overline{\omega}^{D}_{2,-1,2,-2}T^{D}_{2,-2} + \overline{\omega}^{D}_{2,1,2,2}T^{D}_{2,2}, \tag{7}$$

with coefficients as defined above but with the associated scaling factors being $|\kappa^{(1)}_{2,-2,2,2}| = |\kappa^{(1)}_{2,2,2,-2}| = 0.0464$ and $|\kappa^{(1)}_{2,1,2,2}| = |\kappa^{(1)}_{2,-1,2,-2}| = 0.0822$. The low scaling factors are indicative of a relatively slow dipolar-coupling mediate coherence transfer, however, under the conditions of very weak rf irradiation, i.e., $3\omega_r/2$.

The third example of realization of low-power homonuclear dipolar recoupling for high-speed MAS conditions involves the recently introduced EXPORT (EXPonentially mOdulation Recoupling Technique) [7] which uses a double-modulating field to simultaneously remove isotropic and anisotropic chemical shift effects for broadband and high-field performance and ensure heteronuclear decoupling without invoking irradiation at the ^{1}H spins. This method requires quite strong rf irradiation on the ^{13}C (and/or ^{15}N) low-γ rf channels, implying our focus here is to reduce the rf irradiation demands (in this case having ^{1}H decoupling turned on) for high-speed spinning experiments through combination with z-rotational decoupling [29] as provided by CN^{ν}_{n} symmetry-based sequences. The rf field irradiation of the EXPORT experiment takes the form

$$H_{\mathrm{rf}}(t) = CF_{\phi_p} + Be^{-iCtF_{\phi_p}}F_z e^{iCtF_{\phi_p}} \tag{8}$$

where $F_{\phi_p} = I_{1\phi_p} + I_{2\phi_p} = e^{-i\phi_p F_z}(I_{1y} + I_{2y})e^{i\phi_p F_z}$ with $F_z = I_{1z} + I_{2z}$ represents Cartesian operators involving spins I and S, while B and C are angular frequency amplitudes for the rf field. Within the interaction frame of the rf irradiation of the EXPORT-CN^{ν}_{n} experiment

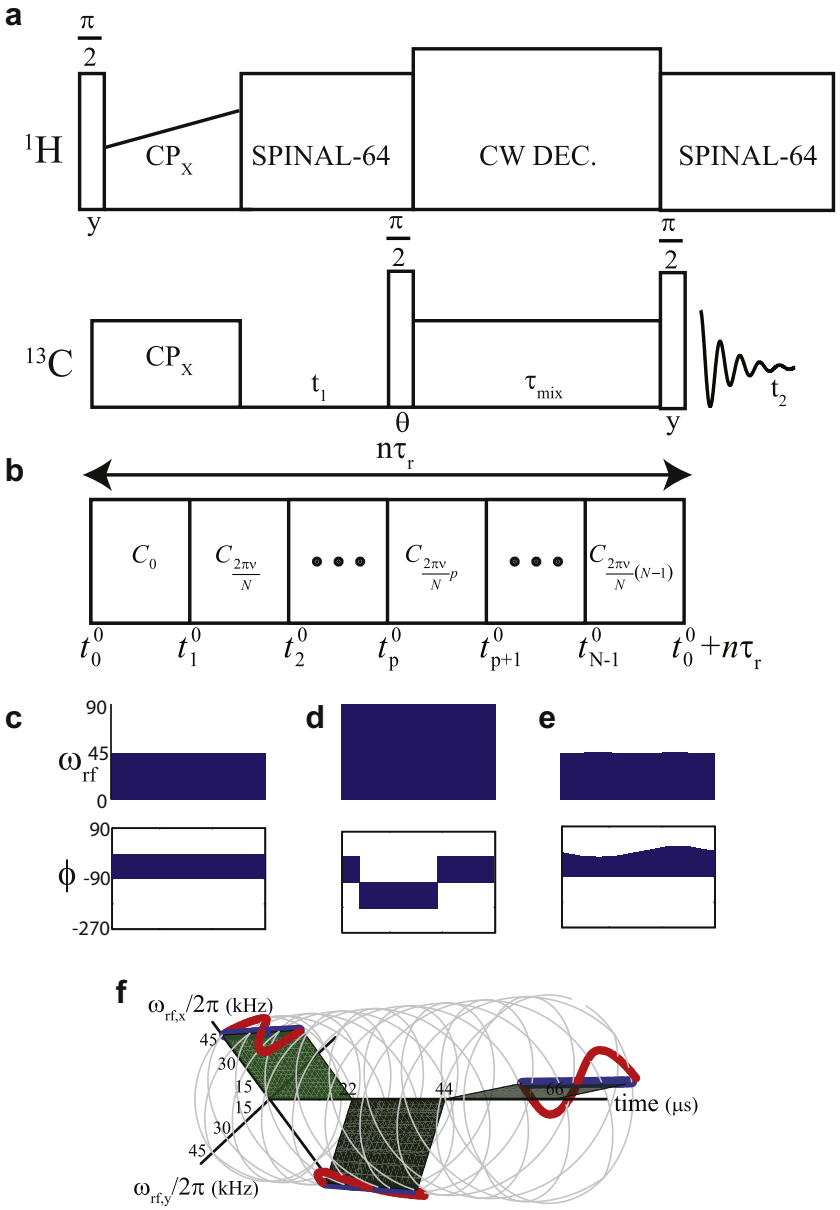

Figure 1. Pulse sequence for 2D solid-state MAS NMR ^{13}C, ^{13}C chemical shift correlation (a) using symmetry-based CN^{ν}_{n} sequences (b) during the mixing part of the pulse sequence. Phase-sensitive spectra are obtained by changing the phase θ according to the TPPI scheme. (c–e) Three different basic elements with specific rf field strengths (kHz, on the vertical axis) corresponding to 30.3 kHz spinning: (c) standard $2\pi_x$ element, (d) POST $\pi/2_x 2\pi_{-y} 3\pi/2_x$ element, and (e) EXPORT elementusing $C = 3\omega_r/2$ and $B = -\omega_r/4$.(f) Rf field trajectories of the basic elements with blue and red lines show rf field strength as function of time for the elements in (c) and (e), respectively. (For interpretation of the references to color in this figure legend, the reader is referred to the web version of this article.)

with the C rf field (Eq. (8)) adjusted to form a full 2π cycle during each individual CN_n^v element, the internal Hamiltonians take the form

$$\tilde{H}^{\Lambda}_{lm\lambda\mu}(t) = \sum_{lm\lambda\mu} \tilde{H}^{\Lambda}_{lm\lambda\mu}(t - t_p^0) e^{i2\pi\frac{p}{N}\left(nm - v\mu - n\mu\frac{B}{\omega_r}\right)}, \tag{9}$$

with

$$\tilde{H}^{\Lambda}_{lm\lambda\mu}(t - t_p^0) = \omega^{\Lambda}_{lm} d^{\lambda}_{\mu 0}(-C(t - t_p^0) e^{\{i\omega_r(t-t_p^0)\left(m-\mu\frac{B}{\omega_r}\right)+i\mu\gamma_0\}} T^{\Lambda}_{\lambda\mu} \tag{10}$$

to a given time t within the p'th pulse sequence element ($t_p^0 \leqslant t \leqslant t_{p+1}^0$). The first-order effective Hamiltonian in Eq. (9) leads to a combined symmetry-based and exponentially-modulated field EXPORT-CN_n^v recoupling selection rule

$$\overline{\tilde{H}}^{\Lambda(1)}_{lm\lambda\mu} = 0 \text{ if } \quad nm - v\mu - \mu n\frac{B}{\omega_r} \neq NZ, \tag{11}$$

where it is required that $nB/\omega_r = Z$ and Z is an integer. Relative to the CN_n^v rule in Eq. (4), the selection rule in Eq. (11) provides additional degrees of freedom for recoupling through the B/ω_r term. Furthermore, additional dependency of the interaction frame Hamiltonian in Eq. (10) may also provide new means for suppression of undesired spin operators.

We focus here on the EXPORT-$C6_4^2$ pulse sequence with $B = -\omega_r/4$ leading to the symmetry $4m - \mu \neq 6Z$ according to the selection rule in Eq. (11). Seen in the light of the low-power $C3$ symmetries discussed above, we note that the EXPORT-$C6_4^2$, being 4 rotor periods long, conveniently may be considered as a consecutive execution of two EXPORT-$C3_2^1$ sequences each of length 2 rotor periods fulfilling very similar rf and time demands as the low-power $C3_2^1\overline{C3}_2^1$ experiment. The EXPORT-$C6_4^2$ pulse sequence recouples the homonuclear dipole–dipole coupling terms $\overline{H}^{(1)}_{2,-2,2,-2}$, $\overline{H}^{(1)}_{2,-2,2,-2}$, $\overline{H}^{(1)}_{2,1,2,-2}$ and $\overline{H}^{(1)}_{2,1,2,-2}$, all having $\mu = \pm 2$ while all terms with $\mu = \pm 1$, including anisotropic shielding, vanish to first-order taking the average Hamiltonian over 4 rotor periods. Through adjustment of the dominant EXPORT field to $C = 3\omega_r/2$, the isotropic chemical shift vanishes via averaging of the $d^{\lambda}_{00}(-C(t - t_p^0)$ term in Eq. (10) while the homonuclear J-coupling term is the same as seen above for the $C3_2^1$ based sequences. For the residual homonuclear dipole–dipole coupling terms, we find through integration the scaling factors $|\kappa^{(1)}_{2,-2,2,-2}| = |\kappa^{(1)}_{2,2,2,2}| = 0.096$ and $|\kappa^{(1)}_{2,1,2,-2}| = |\kappa^{(1)}_{2,-1,2,2}| = 0.150$ for EXPORT-$C6_4^2$ with $B = -\omega_r/4$, being very similar to our findings for the more rf demanding $C3_1^1\overline{C3}_1^1$ experiment and a factor of two better than the rf-power-wise similarly favorable $C3_2^1\overline{C3}_2^1$ experiment. Overall this ensures that the EXPORT-$C6_4^2$ experiment with $B = -\omega_r/4$ and $C = 3\omega_r/2$ provides efficient γ-encoded dipolar recoupling over a relatively broad chemical shift range while maintaining the rf amplitude in the range of $3\omega_r/2$ being compatible with high-speed spinning conditions.

3. Experimental

All experiments were performed on a wide-bore Bruker Avance 400 MHz (9.4 T) NMR spectrometer equipped with a standard triple-resonance 2.5 mm solid-state NMR probe. Simulations were done using the open-source SIMPSON simulation package [21,31,32] using typical chemical shielding and dipolar coupling tensors obtained using SIMMOL [33]. All simulations used powder averaging with 5 γ_{PR} angles and 144 α_{PR}, β_{PR} REPULSION angles [34]. 2,3-$^{13}C_2$-L-alanine was purchased from Isotec. Inc. (Miamisburg, OH). Amyloid fibrils of the fibrillating core decapeptide hIAPP$_{20-29}$ (SNNFGAILSS) of human Islet Amyloid Poly-Peptide (amylin; forming amyloid fibrils in relation to diabetes II) were prepared with uniform ^{13}C,^{15}N-labelling on the FGAIL residues as described previously [4].

4. Results and discussion

The overall pulse scheme for a ^{13}C,^{13}C correlation experiment is illustrated in Figure 1a with specification of a general CN_n^v symmetry-based dipolar recoupling pulse sequence (Figure 1b) using different basic elements (Figure 1c–e) for transfer of ^{13}C coherence between spins within the mixing period of the 2D experiment (Figure 1a). Figure 1f illustrates the rf field trajectory for the basic pulse sequence elements in Figure 1c (blue line) and e (red line). Aimed primarily at fast MAS experiments, the mixing block may be formed by the $C3_1^1\overline{C3}_1^1$, $C3_2^1\overline{C3}_2^1$, or EXPORT-$C6_4^2$ elements introduced above for low-power recoupling. The CN_n^v elements are straightforwardly implemented by adjusting the rf amplitude to

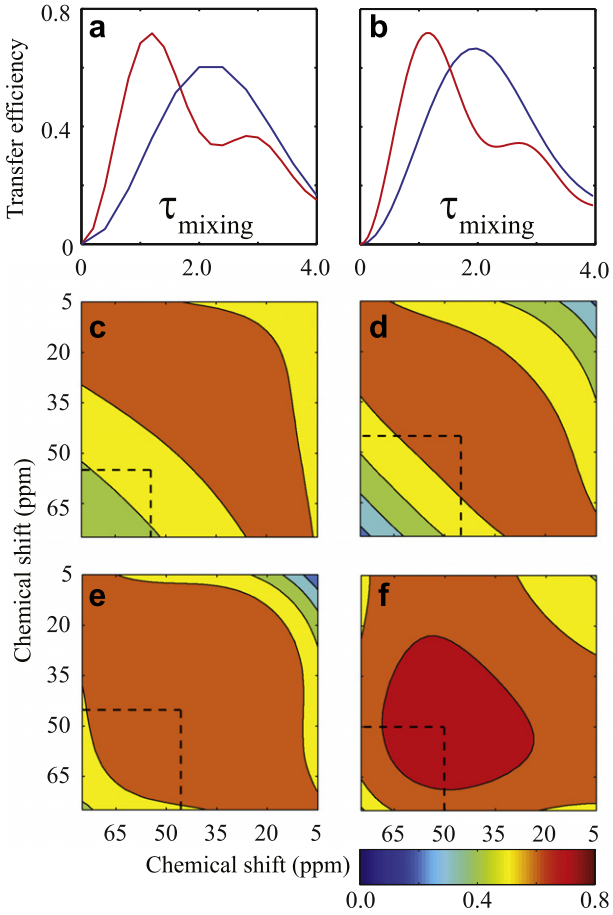

Figure 2. Numerical simulations of the efficiency of ^{13}C–^{13}C coherence transfer between typical aliphatic (e.g., $^{13}C_\alpha$ and $^{13}C_\beta$ in an amino acid residue) as function of excitation time (a and b) and 2D offset variation (c–f). All simulations assume a magnetic field of 16.4 T, spin system parameters (except isotropic chemical shifts) corresponding to the $^{13}C_\alpha$–$^{13}C_\beta$ spin pair of L-alanine (see, e.g., Ref. [22]), and initial spin-operator being I_z on $^{13}C_\alpha$ and the detection operator being S_z on $^{13}C_\beta$. Recoupling sequence, rf field strength, spinning speed parameters for the simulations (a) 10 kHz spinning, ^{13}C rf field strength of 30 kHz corresponding to POST-$C3_2^1\overline{C3}_2^1$ ($\pi/2_x2\pi_{-x}3\pi/2_x$ elements) in blue and $C3_1^1\overline{C3}_1^1$ (2π elements)in red. (b) 30.3 kHz spinning, ^{13}C rf field strength of 45 kHz corresponding to $C3_2^1\overline{C3}_2^1$ (2π element) in blue and EXPORT-$C6_4^2$($C = 3\omega_r/2$ and $B = -\omega_r/4$) in red. (c-f) Offset profiles for the POST-$C3_2^1\overline{C3}_2^1$ ($\pi/2_x2\pi_{-x}3\pi/2_x$ elements) (c) and $C3_1^1\overline{C3}_1^1$ (2π elements) (e) using 10 kHz spinning and $C3_2^1\overline{C3}_2^1$ (2π element) (d) and EXPORT-$C6_4^2$($C = 3\omega_r/2$ and $B = -\omega_r/4$) (f) using 30.3 kHz spinning. (For interpretation of the references to colour in this figure legend, the reader is referred to the web version of this article.)

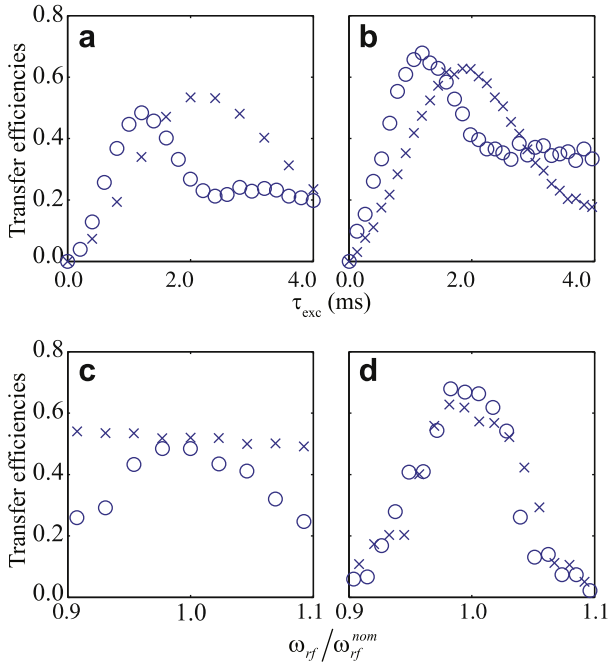

Figure 3. Experimental demonstration of the efficiency of $^{13}C_\alpha$ to $^{13}C_\beta$ polarization transfer obtained for 2,3-$^{13}C_2$-*L*-alanine at 9.4 T as function of (a and b) the mixing time and (c and d) rf mismatch (ratio between actual and nominal rf field strength) using (a and c) POST-$C3_2^1\overline{C3}_2^1$ ($\pi/2_x2\pi_{-x}3\pi/2_x$ elements), 30 kHz rf field strength, 10 kHz spinning (open circles) and $C3_1^1\overline{C3}_1^1$ (2π elements), 30 kHz rf field strength, 10 kHz spinning (crosses), (b and d) $C3_2^1\overline{C3}_2^1$ (2π elements), 45.45 kHz rf field strength, 30.3 kHz spinning (crosses) and EXPORT-$C6_4^2$ ($C = 3\omega_r/2$ and $B = -\omega_r/4$) and 30.3 kHz spinning (open circles).

$N\omega_r/n$ (for 2π elements) or $2N\omega_r/n$ (for standard $2\pi_x2\pi_{-x}$ or POST $\pi/2_x2\pi_{-x}3\pi/2_x$ elements) and using the phase modulation scheme $\phi_p = 2\pi np/N$ ($p = 0,1,...,N-1$) dictated by the symmetry of the sequence. The concatenated element invoked through supercycling is identical to the first CN_n^v element except for addition of π to all phases. The EXPORT building block is implemented (based on Eq. (6)) with amplitude (in angular frequencies) $A(t) = \sqrt{C^2 + B\sin^2(Ct)}$ and phase $\phi(t) = \frac{B}{C}\sin(Ct)$, to which the basic phase of the CN_n^v cycling is added to form the integrated EXPORT-CN_n^v experiment.

The numerical simulations in Figure 2 illustrates the efficiency (relative to unit prior to the element) of typical $^{13}C_\alpha$ to $^{13}C_\beta$ coherence transfers that may be obtained at 16.4 T (700 MHz for protons) as function of excitation time (Figure 2a and b) and chemical shift offsets for the two spins (Figure 2c–f). The simulations in Figure 2a assumed 10 kHz sample spinning and a ^{13}C rf field strength of 30 kHz corresponding to mixing with a POST-$C3_2^1\overline{C3}_2^1$ ($\pi/2_x2\pi_{-x}3\pi/2_x$ elements) shown in blue and $C3_1^1\overline{C3}_1^1$ (2π elements) shown in red. The simulations in Figure 2b assumed 30.3 kHz spinning and a ^{13}C rf field strength of approximately 45 kHz corresponding to mixing with $C3_2^1\overline{C3}_2^1$ (2π element) shown in blue and EXPORT-$C6_4^2$($C = 3\omega_r/2$ and $B = -\omega_r/4$) shown in red. It is evident that the low-power phase-alternated symmetry-based sequences are capable of mediating efficient coherence transfer and the difference in the dipolar scaling factors as discussed in the theory section is confirmed numerically leading to optimal polarization transfer for mixing times of 2.0 ms (POST-$C3_2^1\overline{C3}_2^1$) and 1.2 ms ($C3_1^1\overline{C3}_1^1$). Addressing high-speed spinning conditions, the maximum coherence transfer efficiency exceeds 70% for EXPORT-$C6_4^2$ with a very fast buildup rate (1.12 ms) as compared to 1.98 ms for $C3_2^1\overline{C3}_2^1$. Figures 2c–f provide 2D offset profiles for POST-$C3_2^1\overline{C3}_2^1$ ($\pi/2_x2\pi_{-x}3\pi/2_x$ elements) in Figure 2c and $C3_1^1\overline{C3}_1^1$ (2π elements) in Figure 2e both at 10 kHz spinning. The corresponding profiles for $C3_2^1\overline{C3}_2^1$ (2π element) in Figure 2d and EXPORT-$C6_4^2$ ($C = 3\omega_r/2$ and $B = -\omega_r/4$) in Figure 2f are obtained for conditions of 30.3 kHz spinning. It is evident that all sequences provide efficient polarization transfer over the full aliphatic region

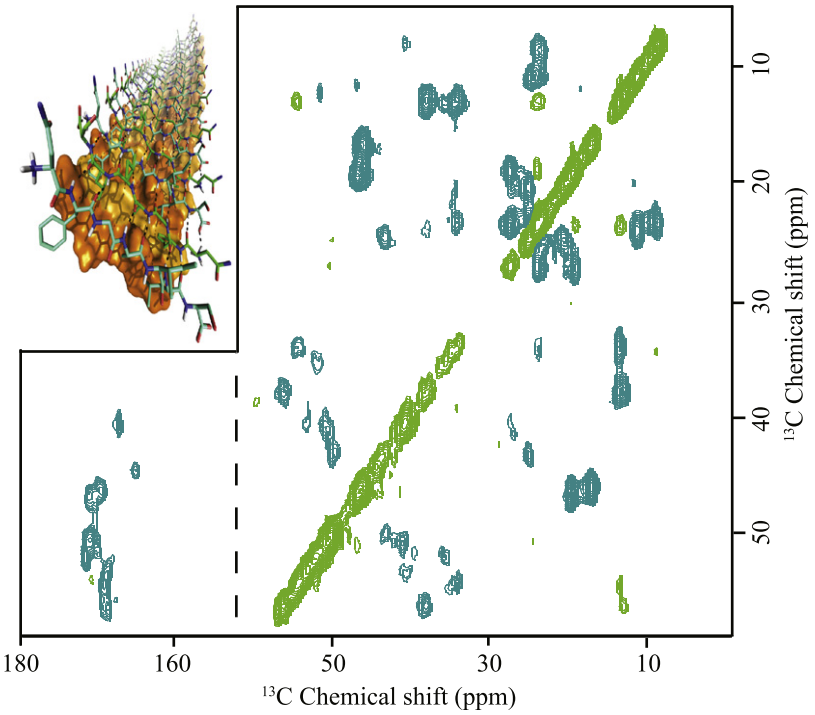

Figure 4. Experimental 2D ^{13}C–^{13}C chemical shift correlation spectrum of hIAPP$_{20-29}$ amyloid fibrils labeled uniformly with ^{13}C and ^{15}N in the FGAIL part of the decapeptide. The spectrum was recorded at 9.4 T with 30.3 kHz sample spinning and mixing using EXPORT-$C6_4^2$ ($C/2\pi$ = 45.45 kHz and $B/2\pi$ = 15.15 kHz). The spectra were acquired using 3 s relaxation delay, rf field strengths of 139 kHz and approximately 46 kHz on the ^1H and ^{13}C channels, respectively, using 400 ms ramped (^1H channel, 20% increase over the initial value with the center at the specified rf field strength), 1.056 ms mixing, 168 number of scans for each of the 128 t_1 increments.

(even for high-field applications) with the highest efficiency observed for the EXPORT-$C6_4^2$ sequence.

Using 2,3-$^{13}C_2$-*L*-alanine as a simple model system, Figure 3 shows a series of experimental $^{13}C_\alpha$ to $^{13}C_\beta$ polarization transfer efficiencies (comparing peak intensities for $^{13}C_\beta$ relative to the initial $^{13}C_\alpha$ state) obtained using POST-$C3_2^1\overline{C3}_2^1$ ($\pi/2_x 2\pi_{-x} 3\pi/2_x$ element) and $C3_1^1\overline{C3}_1^1$ (2π element) with 10 kHz spinning (Figure 3a) as well as $C3_2^1\overline{C3}_2^1$ (2π element) and EXPORT-$C6_4^2$ ($C = 3\omega_r/2$ and $B = -\omega_r/4$) with 30.3 kHz spinning. The former experiments provide a maximum transfer of around 50%, while $C3_2^1\overline{C3}_2^1$ and EXPORT-$C6_4^2$ provides 62.5% and 67.5%, respectively, all using mixing times very similar to those predicted numerically. Figures 3c and d show experimental rf mismatch curves for the four experiments, revealing that they all are quite robust towards rf inhomogeneity and rf misadjustments with particularly robustness observed for the POST-$C3_2^1\overline{C3}_2^1$ experiment. We note that the same robustness may be obtained for the $C3_2^1\overline{C3}_2^1$ and EXPORT-$C6_4^2$ experiments upon replacing the 2π basic element with the POST $\pi/2_x 2\pi_{-x} 3\pi/2_x$ element, however, at the expense of increasing the rf field strength from $1.5\omega_r$ to $3\omega_r$.

Figure 4 shows a 2D ^{13}C, ^{13}C carbon chemical shift correlation spectrum for of hIAPP$_{20-29}$ amyloid fibrils uniformly-^{13}C, ^{15}N labeled at the FGAIL residues and recorded at 9.4 T using 30.3 kHz MAS. The EXPORT-$C6_4^2$ pulse sequence was used in the mixing element of the 2D pulse sequence in Figure 1a. This spectrum clearly demonstrates the attractive broadband features of the low-power ($C = 3\omega_r/2$) EXPORT-$C6_4^2$ combining the attractive features of EXPORT with symmetry-based homonuclear recoupling.

5. Conclusions

In conclusion, we have demonstrated the feasibility of designing symmetry-based and exponentially-modulated dipolar recoupling experiments with low rf power demands relative to previous realizations. This is accomplished using supercycling to eliminate non-desired first-order dipolar coupling and chemical shift effective Hamiltonians, as well as second-order cross-terms involved dipole–dipole coupling and chemical shielding interactions, and introduction of new dipolar recoupling symmetry rules by intertwining EXPORT and symmetry-based recoupling. The resulting pulse sequence proves to be very efficient for transfer of coherence between, e.g., aliphatic carbons in proteins, under high-speed spinning condition or situations where strong rf fields are not desirable (e.g., for lossy samples or expensive protein samples being sensitive to temperature variation due to rf induced heating) and should find immediate important applications as part of the pulse sequence tool box in biological solid-state NMR spectroscopy.

Acknowledgements

We acknowledge support from the Danish National Research Foundation, the Danish Center for Scientific Computing at Aarhus University, and the Villum-Kann Rasmussen foundation. We thank Prof. N. Khaneja for helpful suggestions, and Dr. E. H. Nielsen for synthesizing the labeled hIAPP$_{20-29}$ peptide.

References

[1] M. Etzkorn, S. Martell, O.C. Andronesi, K. Seidel, M. Engelhard, M. Baldus, Angew. Chem. Int. Ed. 46 (2007) 459.
[2] S.D. Cady, K. Schmidt-Rohr, J. Wang, C.S. Soto, W.F. DeGrado, M. Hong, Nature 463 (2010) 689.
[3] C. Wasmer, A. Lange, H. Van Melckebeke, A.B. Siemer, R. Riek, B.H. Meier, Science 319 (2008) 1523.
[4] J.T. Nielsen et al., Angew. Chem. Int. Ed. 48 (2009) 2118.
[5] G. De Paepe, M.J. Bayro, J. Lewandowski, R.G. Griffin, J. Am. Chem. Soc. 128 (2006) 1776.
[6] M.J. Bayro, R. Ramachandran, M.A. Caporini, M.T. Eddy, R.G. Griffin, J. Chem. Phys. 128 (2008) 052321.
[7] A.B. Nielsen, L.A. Straasø, A.J. Nieuwkoop, C.M. Rienstra, M. Bjerring, N.C. Nielsen, J. Phys. Chem. Lett. 1 (2010) 1952.
[8] M. Bjerring, A.B. Nielsen, Z. Tosner, N.C. Nielsen, Chem. Phys. Lett. 494 (2010) 326.
[9] R. Verel, M. Ernst, B.H. Meier, J. Magn. Reson. 150 (2001) 81.
[10] K. Takegoshi, S. Nakamura, T. Terao, J. Chem. Phys. 118 (2003) 2325.
[11] I. Scholz, B.H. Meier, M. Ernst, Chem. Phys. Lett. 479 (2009) 296.
[12] M. Weingarth, G. Bodenhausen, P. Tekely, Chem. Phys. Lett. 488 (2010) 10.
[13] N. Khaneja, N.C. Nielsen, J. Chem. Phys. 128 (2008) 015103.
[14] L.A. Straasø, M. Bjerring, N. Khaneja, N.C. Nielsen, J. Chem. Phys. 130 (2009) 225103.
[15] J. Lin, M.J. Bayro, R.G. Griffin, N. Khaneja, J. Magn. Reson. 199 (2009) 247.
[16] L.A. Straasø, N.C. Nielsen, J. Chem. Phys. 133 (2010) 064501.
[17] C.T. Kehlet, A.C. Sivertsen, M. Bjerring, T.O. Reiss, N. Khaneja, S.J. Glaser, N.C. Nielsen, J. Am. Chem. Soc. 126 (2004) 10202.
[18] C. Kehlet, T. Vosegaard, N. Khaneja, S.J. Glaser, N.C. Nielsen, Chem. Phys. Lett. 414 (2005) 204.
[19] C. Kehlet et al., J. Magn. Reson. 188 (2007) 216.
[20] A.B. Nielsen, M. Bjerring, J.T. Nielsen, N.C. Nielsen, J. Chem. Phys. 131 (2009) 025101.
[21] Z. Tosner, T. Vosegaard, C. Kehlet, N. Khaneja, S.J. Glaser, N.C. Nielsen, J. Magn. Reson. 197 (2009) 120.
[22] N.C. Nielsen, H. Bildsøe, H.J. Jakobsen, M.H. Levitt, J. Chem. Phys. 101 (1994) 1805.
[23] Y.K. Lee, N.D. Kurur, M. Helmle, O.G. Johannessen, N.C. Nielsen, M.H. Levitt, Chem. Phys. Lett. 242 (1995) 304.
[24] M. Hohwy, H.J. Jakobsen, M. Eden, M.H. Levitt, N.C. Nielsen, J. Chem. Phys. 108 (1998) 2686.
[25] M. Eden, M.H. Levitt, J. Chem. Phys. 111 (1999) 1511.
[26] A. Brinkmann, M. Eden, M.H. Levitt, J. Chem. Phys. 112 (2000) 8539.
[27] M.H. Levitt, J. Chem. Phys. 128 (2008) 052205.
[28] C. Herbst et al., NMR 44 (2009) 175.
[29] M. Hohwy, N.C. Nielsen, J. Chem. Phys. 109 (1998) 3780.
[30] M. Hohwy, N.C. Nielsen, J. Chem. Phys. 106 (1997) 7571.
[31] M. Bak, J.T. Rasmussen, N.C. Nielsen, J. Magn. Reson. 147 (2000) 296.
[32] T. Vosegaard, A. Malmendal, N.C. Nielsen, Monatsh. Chem. 133 (2002) 1555.
[33] M. Bak, R. Schultz, T. Vosegaard, N.C. Nielsen, J. Magn. Reson. 154 (2002) 28.
[34] M. Bak, N.C. Nielsen, J. Magn. Reson. 125 (1997) 132.